patients with non-small cell lung cancer. Lung Cancer 2002, 36:143–150
16. Mascaux C, Martin B, Paesmans M, Verdebout JM, Verhest A, Vermylen P, Bosschaerts T, Ninane V, Sculier JP: Expression of thrombospondin in non-small cell lung cancer. Anticancer Res 2002, 22:1273–1277
17. Dudek AZ, Mahaseth H: Circulating angiogenic cytokines in patients with advanced non-small cell lung cancer: correlation with treatment response and survival. Cancer Invest 2005, 23:193–200
18. Watanabe K, Hasegawa Y, Yamashita H, Shimizu K, Ding Y, Abe M, Ohta H, Imagawa K, Hojo K, Maki H, Sonoda H, Sato Y: Vasohibin as an endothelium-derived negative feedback regulator of angiogenesis. J Clin Invest 2004, 114:898–907
19. Shibuya T, Watanabe K, Yamashita H, Shimizu K, Miyashita H, Abe M, Moriya T, Ohta H, Sonoda H, Shimosegawa T, Tabayashi K, Sato Y: Isolation and characterization of vasohibin-2 as a homologue of VEGF-inducible endothelium-derived angiogenesis inhibitor vasohibin. Arterioscler Thromb Vasc Biol 2006, 26:1051–1057
20. Shimizu K, Watanabe K, Yamashita H, Abe M, Yoshimatsu H, Ohta H, Sonoda H, Sato Y: Gene regulation of a novel angiogenesis inhibitor, vasohibin, in endothelial cells. Biochem Biophys Res Commun 2005, 327:700–706
21. Koizumi T, Abe M, Yamakuni T, Ohizumi Y, Hitotsuyanagi Y, Takeya K, Sato Y: Metronomic scheduling of a cyclic hexapeptide Ra-VII for anti-angiogenesis, tumor vessel maturation and anti-tumor activity. Cancer Sci 2006, 97:665–674
22. Kimura H, Miyashita H, Suzuki Y, Kobayashi M, Watanabe K, Sonoda H, Ohta H, Fujiwara T, Shimosegawa T, Sato Y: Distinctive localization and opposed roles of vasohibin-1 and vasohibin-2 in the regulation of angiogenesis. Blood 2009, 113:4810-4818
23. Yamashita H, Abe M, Watanabe K, Shimizu K, Moriya T, Sato A, Satomi S, Ohta H, Sonoda H, Sato Y: Vasohibin prevents arterial neointimal formation through angiogenesis inhibition. Biochem Biophys Res Commun 2006, 345:919–925
24. Li G, Tian L, Hou JM, Ding ZY, He QM, Feng P, Wen YJ, Xiao F, Yao B, Zhang R, Peng F, Jiang Y, Luo F, Zhao X, Zhang L, Zhou Q, Wei YQ: Improved therapeutic effectiveness by combining recombinant CXC chemokine ligand 10 with Cisplatin in solid tumors. Clin Cancer Res 2005, 11:4217–4224
25. Bardella C, Dettori D, Olivero M, Coltella N, Mazzone M, Di Renzo MF: The therapeutic potential of hepatocyte growth factor to sensitize ovarian cancer cells to cisplatin and paclitaxel in vivo. Clin Cancer Res 2007, 13:2191–2198
26. Kim SJ, Rabbani ZN, Dewhirst MW, Vujaskovic Z, Vollmer RT, Schreiber EG, Oosterwijk E, Kelley MJ: Expression of HIF-1α, CA IX, VEGF, and MMP-9 in surgically resected non-small cell lung cancer. Lung Cancer 2005, 49:325–335
27. McDonald DM, Foss AJ: Endothelial cells of tumor vessels: abnormal but not absent. Cancer Metastasis Rev 2000, 19:109–120
28. Bodey B, Bodey B Jr, Siegel SE, Kaiser HE: Immunocytochemical detection of endoglin is indicative of angiogenesis in malignant melanoma. Anticancer Res 1998, 18:2701–2710
29. Petrovic N, Bhagwat SV, Ratzan WJ, Ostrowski MC, Shapiro LH: CD13/APN transcription is induced by RAS/MAPK-mediated phosphorylation of Ets-2 in activated endothelial cells. J Biol Chem 2003, 278:49358–49368
30. St Croix B, Rago C, Velculescu V, Traverso G, Romans KE, Montgomery E, Lal A, Riggins GJ, Lengauer C, Vogelstein B, Kinzler KW: Genes expressed in human tumor endothelium. Science 2000, 289:1197–1202
31. van Beijnum JR, Dings RP, van der Linden E, Zwaans BM, Ramaekers FC, Mayo KH, Griffioen AW: Gene expression of tumor angiogenesis dissected: specific targeting of colon cancer angiogenic vasculature. Blood 2006, 108:2339–2348
32. Seaman S, Stevens J, Yang MY, Logsdon D, Graff-Cherry C, St Croix B: Genes that distinguish physiological and pathological angiogenesis. Cancer Cell 2007, 11:539–554
33. Yoshinaga K, Ito K, Moriya T, Nagase S, Takano T, Niikura H, Yaegashi N, Sato Y: Expression of vasohibin as a novel endothelium-derived angiogenesis inhibitor in endometrial cancer. Cancer Sci 2008, 99:914–919
34. Hanahan D, Folkman J: Patterns and emerging mechanisms of the angiogenic switch during tumorigenesis. Cell 1996, 86:353–364
35. Jain RK: Normalization of tumor vasculature: an emerging concept in antiangiogenic therapy. Science 2005, 307:58–62

blood

2009 113: 4810-4818
Prepublished online Feb 9, 2009;
doi:10.1182/blood-2008-07-170316

Distinctive localization and opposed roles of vasohibin-1 and vasohibin-2 in the regulation of angiogenesis

Hiroshi Kimura, Hiroki Miyashita, Yasuhiro Suzuki, Miho Kobayashi, Kazuhide Watanabe, Hikaru Sonoda, Hideki Ohta, Takashi Fujiwara, Tooru Shimosegawa and Yasufumi Sato

Blood (print ISSN 0006-4971, online ISSN 1528-0020), is published semimonthly by the American Society of Hematology, 1900 M St, NW, Suite 200, Washington DC 20036.

Distinctive localization and opposed roles of vasohibin-1 and vasohibin-2 in the regulation of angiogenesis

Hiroshi Kimura,[1,2] Hiroki Miyashita,[1] Yasuhiro Suzuki,[1] Miho Kobayashi,[1] Kazuhide Watanabe,[1] Hikaru Sonoda,[3] Hideki Ohta,[3] Takashi Fujiwara,[4] Tooru Shimosegawa,[2] and Yasufumi Sato[1]

[1]Department of Vascular Biology, Institute of Development, Aging, and Cancer, Tohoku University, Sendai; [2]Department of Gastroenterology, Tohoku University Graduate School of Medicine, Sendai; [3]Discovery Research Laboratories, Shionogi and Co, Osaka; and [4]Department of Biological Resources, Integrated Center for Science (INCS), Ehime University, Shitsukawa, Ehime, Japan

We recently isolated a novel angiogenesis inhibitor, vasohibin-1, and its homologue, vasohibin-2. In this study we characterize the role of these 2 molecules in the regulation of angiogenesis. In a mouse model of subcutaneous angiogenesis, the expression of endogenous vasohibin-1 was low in proliferating ECs at the sprouting front but high in nonproliferating endothelial cells (ECs) in the termination zone. In contrast, endogenous vasohibin-2 was preferentially expressed in mononuclear cells mobilized from bone marrow that infiltrated the sprouting front. When applied exogenously, vasohibin-1 inhibited angiogenesis at the sprouting front where endogenous vasohibin-1 was scarce but did not influence vascularity in the termination zone where endogenous vasohibin-1 was enriched. Exogenous vasohibin-2 prevented the termination of angiogenesis in the termination zone and increased vascularity in this region. Angiogenesis was persistent in the termination zone in the *vasohibin-1* knockout mice, whereas angiogenesis was deficient at the sprouting front in the *vasohibin-2* knockout mice. Supplementation of deficient proteins normalized the abnormal patterns of angiogenesis in the vasohibin knockout mice. These results indicate that vasohibin-1 is expressed in ECs in the termination zone to halt angiogenesis, whereas vasohibin-2 is expressed in infiltrating mononuclear cells in the sprouting front to promote angiogenesis. (Blood. 2009; 113:4810-4818)

Introduction

Angiogenesis, or the formation of new capillaries, is a key event in various developmental or remodeling processes that take place under physiologic and pathologic conditions. Angiogenesis is a dynamic phenomenon that involves sequential processes. The initial event is the detachment of mural pericytes from preexisting vessels for vascular destabilization. Subsequently, specialized endothelial cells (ECs) at the tip of sprout, called tip cells, degrade the basement membrane and extracellular matrices and actively migrate. The stalk cells follow the tip cells, proliferate, and form tubes. Finally, pericytes reattach to the new vessels as they mature. Through these processes, a new hierarchical vascular architecture will be constructed.[1]

The local balance between angiogenesis stimulators and inhibitors determines whether angiogenesis will be switched on. Numerous endogenous angiogenesis inhibitors are found in the body and play distinctive roles.[2] For example, molecules such as pigment epithelium-derived factor,[3,4] chondromodulin-1,[5,6] and maspin[7,8] are localized extrinsic to the vasculature and block the intrusion of new vessels as functional barriers. Thrombospondin-1 and thrombospondin-2 are deployed mainly by platelets and turn the angiogenic switch off.[9] Moreover, several angiogenesis inhibitors, including endostatin and tumstatin, are generated by the degradation of the basement membrane during angiogenesis.[10] Besides them, ECs themselves have the capacity to synthesize certain inhibitors that autoregulate angiogenesis.[2]

By searching for novel and functional vascular endothelial growth factor (VEGF)–inducible molecules in ECs, we isolated one angiogenesis inhibitor and named it vasohibin-1 (VASH1).[11] VASH1 is induced in cultured ECs by representative angiogenic growth factors, such as VEGF and fibroblast growth factor 2 (FGF-2), and is detected selectively in ECs at the site of angiogenesis in vivo.[11] The inducible expression of VASH1 in ECs is impaired by tumor necrosis factor-α, interleukin-1, or hypoxia.[11,12] Human VASH1 protein is composed of 365 amino acid residues. VASH1 lacks a classical secretion signal sequence but is released extracellulary, indicating that VASH1 is an unconventional secretory protein.[11,13] When applied exogenously, VASH1 inhibits the migration and proliferation of ECs stimulated with either VEGF or FGF-2.[11] This inhibitory effect is not due to the inactivation of growth factor signals, because VASH1 does not affect VEGF receptor 2 or ERK1/2 phosphorylation in ECs on VEGF simulation.[11] VASH1 exerts antiangiogenic activity under various pathologic conditions such as those of tumors, retinal neovascularization, and arterial intimal thickening, implying a possible clinical application.[11,14,15]

Through a DNA sequence search of genomic databases, we found one gene homologous to VASH1 and named it vasohibin-2 (VASH2).[16] The genes for human *VASH1* and *VASH2* are located on chromosome 14q24.3 and 1q32.3, respectively.[17] Human vasohibin-2 is composed of 355 amino acid residues, and the overall homology between human VASH1 and VASH2 is 52.5% at

Submitted July 23, 2008; accepted January 27, 2009. Prepublished online as *Blood* First Edition paper, February 9, 2009; DOI 10.1182/blood-2008-07-170316.

The online version of this article contains a data supplement.

The publication costs of this article were defrayed in part by page charge payment. Therefore, and solely to indicate this fact, this article is hereby marked "advertisement" in accordance with 18 USC section 1734.

the amino acid level. Similar to VASH1, any known functional motifs are found in the primary structure of VASH2.

The expression of VASH2 in cultured ECs is very low and is not inducible, but VASH1 and VASH2 proteins are comparably detected in ECs in the developing organs of embryos.[16] We have shown that VASH1 and VASH2 are diffusely expressed in ECs in embryonic organs during mid-gestation. After that time point, they become faint but persisted to a certain extent from late-gestation to neonate. Nevertheless, the function of these 2 molecules remained to be elucidated.

Here, we examined the roles of VASH1 and VASH2 in the regulation of postnatal angiogenesis in detail. For this purpose, we used a simple and reproducible model of postnatal angiogenesis in mice. To our surprise, the spatiotemporal expression patterns of VASH1 and VASH2 were distinct, with VASH1 present in ECs where angiogenesis terminated and with VASH2 present in bone marrow–derived mononuclear cells (MNCs) at the sprouting front. Furthermore, a loss-of-function experiment using knockout mice, as well as a gain-of-function experiment using adenovirus-mediated gene transfer, showed that VASH1 and VASH2 play distinctive roles in the regulation of angiogenesis.

Methods

Mouse model of hypoxia-mediated subcutaneous angiogenesis

All animal studies were reviewed and approved by the committee for animal study in the Institute of Development, Aging, and Cancer at Tohoku University.

A mouse model of subcutaneous angiogenesis was performed in accordance with the method described by Tepper et al.[18] Briefly, after anesthetization, bilateral incisions (2.5 cm in length and 1.25 cm in distance) were made on the dorsal skin of male C57BL/6 mice (Clea, Tokyo, Japan) that penetrated the cutis, dermis, and underlying adipose tissue. A silicon sheet was inserted beneath the flap, and the incisions were closed. In some experiments, adenovirus vector encoding the human *VASH1* gene (AdVASH1),[11] AdVASH2, or adenoviral vector encoding *β-galactosidase* gene (AdLacZ; 10^9 plaque-forming units was injected into the tail vein.[15] AdVASH2 was prepared in accordance with the method described.[11] Seven days after skin surgery, the mice were killed, and the skin flaps were collected for histologic analyses.

For the detection of hypoxic areas, mice were intravenously injected with pimonidazole (Chemicon International, Temecula, CA) 30 minutes before collecting the flap. Hypoxic areas were detected with the Hypoxyprobe-1 mAb1 (Chemicon International).

Generation of *VASH1* and *VASH2* knockout mice

For the construction of the *VASH1* targeting vector, a 7.6-kb genomic fragment upstream of exon 1 and a 2.4-kb genomic fragment downstream of exon 2 were subcloned. The region was designed such that the short homology arm (SA) extends 2.4 kb to 5′ end of loxP/FRT flanked Neo cassette, and the long homology arm (LA) starts at the 3′ side of loxP/FRT flanked Neo cassette. For the construction of the *VASH2* targeting vector, a 7.8-kb genomic fragment upstream of exon 3 and a 2.4-kb genomic fragment downstream of exon 3 were subcloned. The region was designed such that the SA extended 2.4 kb to the 5′ side of the Neo cassette, and the LA started at the 5′ side of LacZ cassette. The loxP/FRT flanked Neo cassette replaced 6.6 kb of the *VASH1* gene, including exon 1 (including the ATG start codon), whereas exon 3 of the *VASH2* gene was replaced with the LacZ/Neo cassette.

Targeted alleles were generated by homologous recombination in embryonic stem (ES) cells of C57BL/6 background. The ES cells carrying each of the targeted alleles were injected into C57BL/6 mouse blastocysts to produce chimeric mice. Chimeras were mated with C57BL/6 females to obtain F1 mice carrying each of the targeted alleles.

Immunohistologic analysis

For immunohistochemical analysis of the skin flap, specimens were frozen in OCT compound (Sakura, Tokyo, Japan), sliced into 10-μm sections, and fixed in methanol for 20 minutes at −20°C. Primary antibody reactions were performed at a dilution of 1:200 for CD31 (rat anti–mouse CD31 mAb; Research Diagnosis, Flanders, NJ), α smooth muscle actin (αSMA) (mouse anti–mouse αSMA mAb; Sigma-Aldrich, St Louis, MO), lymphatic vessel endothelial hyaluronate receptor 1 (LYVE-1; rabbit anti–mouse LYVE-1 polyclonal Ab; Acris Antibodies, Himmelreich, Germany), PCNA (mouse anti–mouse PCNA mAb; Santa Cruz Biotechnology, Santa Cruz, CA), CD11b (goat anti–mouse CD11b polyclonal Ab; Santa Cruz Biotechnology), and macrophage-specific antigen F4/80 (rat anti–mouse F4/80 mAb; Acris Antibodies) and at 1:400 for mouse VASH1 (rabbit anti–mouse VASH1 polyclonal Ab)[16] and VASH2 (rabbit anti–mouse VASH 2 polyclonal Ab)[16] overnight at 4°C. Specificities of anti–mouse VASH1 and anti–mouse VASH2 antibodies have been shown previously.[16] Secondary antibody reactions were performed at a dilution of 1:1500 of the appropriate Alexa 488–, Alexa 568–, or Alexa 594–conjugated donkey secondary Abs (Molecular Probes, Eugene, OR) for 1 hour at room temperature. The vascular luminal area was calculated from 5 different high-power fields.

For whole-mount immunohistochemical analysis of ear skin, the ear skin was prepared according to the method described by Oike et al.[19] Briefly, ear skin was fixed with 4% paraformaldehyde in PBS for 2 hours, permeabilized with methanol, and blocked in 5% sheep serum in 0.3% Triton X-100 (Sigma-Aldrich) in PBS. Primary antibodies and secondary antibodies were incubated overnight at 4°C.

All the samples were analyzed with a Fluoview FV1000 confocal fluorescence microscope (Olympus, Tokyo, Japan) with an UPLSAP 10× or 40× objective lens at room temperature. Fluorochromes used were Alexa 488, Alexa 594, fluorescein isothiocyanate (FITC), or green fluorescent protein (GFP). We used Olympus Fluoview software.

Scanning electron microscopy

Ear skin was obtained and fixed with 3% glutaraldehyde in 0.1 M phosphate buffer (pH 7.4). The method of scanning electron microscopy (SEM) observation was as previously reported.[20] In brief, the specimens were treated with 1% to 2% sodium hypochlorite solution for 45 to 100 seconds, hydrolyzed with 8N HCl for 30 minutes, postfixed with 1% OsO_4, treated with 1% tannic acid solution, and again with 1% OsO_4. After a brief rinse, the specimens were dehydrated through a graded series of ethanol, immersed in t-butyl alcohol, freeze-dried, coated with platinum, and observed with an SEM (Hitachi S-800; Hitachi, Tokyo, Japan).

Detection of vessel perfusion

For the detection of blood vessels with perfusion, mice were infused with FITC-labeled concanavalin A (Sigma-Aldrich) by intracardiac injection before the collection of skin flap. Thereafter, samples were analyzed using a confocal fluorescence microscope (Olympus).

Bone marrow transplantation

Wild-type mice were lethally irradiated with 1 dose of 9 Gy. Thereafter, bone marrow cells harvested from GFP-mice (generous gift from Dr Okabe, Osaka University, Osaka, Japan) that had been purified by density centrifugation (Ficoll-paque PLUS; Amersham Biosciences, Uppsala, Sweden), were transplanted into the wild-type mice (5×10^6 cells/animal). All the recipient mice were given a minimum of 6 weeks of rest to allow for complete bone marrow reconstitution. The engraftment efficiency was determined by fluorescence-activated cell sorting (FACS; FACS Vantage; Becton Dickinson, San Jose, CA) for GFP expression in the bone marrow of mice receiving transplants of GFP-positive bone marrow cells.

Cells

Human umbilical vein endothelial cells (HUVECs) were obtained from KURABO Industries (Osaka, Japan) and were cultured on type-1 collagen–coated dishes (IWAKI, Chiba, Japan) in 10% fetal bovine serum (FBS)/

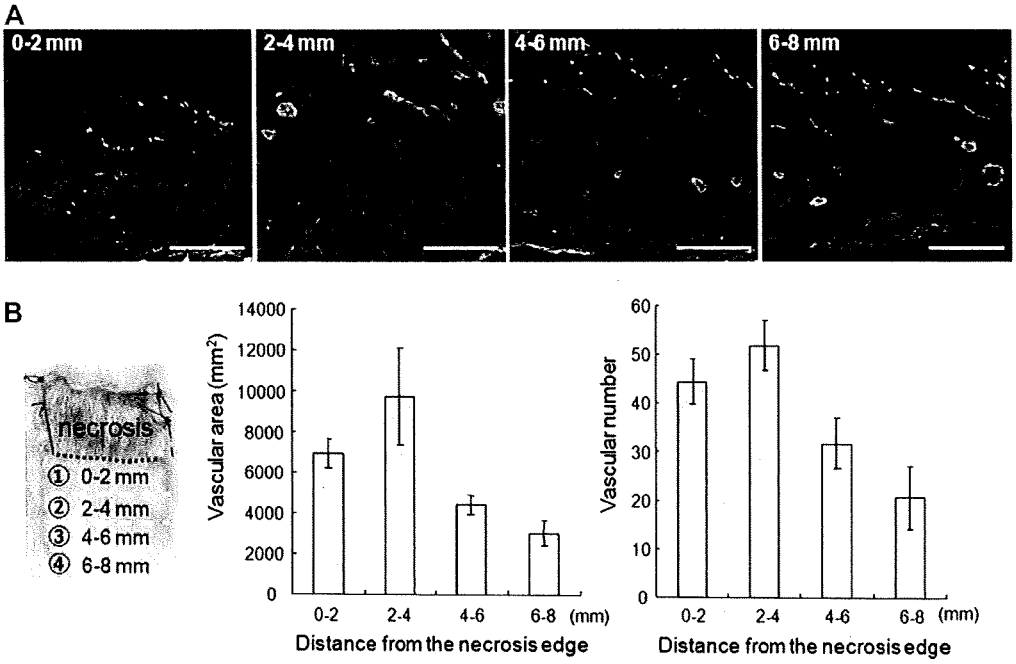

Figure 1. New vessel distribution in the skin flap. (A) The vascular distribution in the skin flap was observed in areas at every 2-mm interval from the necrotic edge. CD31 (red) is a marker for ECs, and αSMA (green) is a marker for mural cells. Scale bars are 200 μm. (B) The dashed line indicates the necrotic edge. The vascular area and vascular density per high-power field were determined from every 2-mm interval from the necrotic edge. Data are expressed as the means and SDs of each area.

endothelial basal medium (Clonetics, Walkersville, MD). THP-1, a human monocytic cell leukemia cell line was obtained from the Cell Resource Center for Biomedical Research at our institute. THP-1 cells were cultured in 10% FBS/RPMI 1640 (Nissui Pharmaceutical, Tokyo, Japan). GM7373, a chemically immortalized bovine aortic endothelial cell line, was cultured in Dulbecco modified Eagle medium (Nissui Pharmaceutical) supplemented with 10% FCS. MS1, an immortalized cell line with a SV40 large T antigen from mouse pancreatic ECs, was purchased from ATCC (Manassas, VA) and were cultured in αMEM (Invitrogen, Carlsbad, CA) supplemented with 10% FCS. All the cells were cultured at 37°C in a humidified atmosphere with 5% CO_2.

Reverse transcriptase-polymerase chain reaction analysis

Total RNA was extracted from HUVECs and THP-1 cells by the AGPC method using ISOGEN (Nippon Gene, Toyama, Japan) according to the manufacturer's instructions. Total tissue RNA was extracted from several organs of male BALB/c mice at 4 weeks or from placentas of female BALB/c mice by the AGPC method using ISOGEN-LS (Nippon Gene). First-strand cDNA was generated using a first-strand cDNA synthesis kit for reverse transcriptase–polymerase chain reaction (RT-PCR; Roche Diagnostics, Mannheim, Germany). RT-PCR was performed with a DNA thermal cycler (Takara, Tokyo, Japan). PCR conditions consisted of an initial denaturation step at 95°C for 10 minutes followed by 40 cycles consisting of 15 seconds at 95°C, 5 seconds at an indicated annealing temperature, and 15 seconds at 72°C. The primer pairs used were as follows: mouse β-actin forward, 5-ACAATGAGCTGCGTGTGGCT, and reverse, 5-TCTCCTTA-ATGTCACGCACGA (annealing temperature 58°C); mouse VASH1 forward, 5-AGATCCCCATACCGAGTGTG, and reverse, 5-GGGCCTCTTT-GGTCATTTCC (annealing temperature 58°C); mouse VASH2 forward, 5′-ATGCCTTGAAGCTGTCATCC, and reverse, 5′-TGGCATATTTCTC-CAGCTCC (annealing temperature 60°C). PCR products were analyzed by 1% or 1.5% agarose gel electrophoresis.

Quantitative real-time RT-RCR

Total RNA was extracted from the skin flap using the RNeasy Mini Kit (QIAGEN, Valencia, CA) according to the manufacturer's instructions. First-strand cDNA was generated with a first-strand cDNA synthesis kit for RT-PCR (Roche Diagnostics). Quantitative real-time RT-PCR was performed with the use of a Light Cycler System (Roche Diagnostics) according to the manufacturer's instructions. The amount of PCR product was measured as a fluorescence signal that was proportional to the amount of the specific target sequence present. PCR conditions consisted of an initial denaturation step at 95°C for 10 minutes, followed by 40 cycles consisting of 15 seconds at 95°C, 5 seconds at an indicated annealing temperature, and 15 seconds at 72°C. The primer pairs used were as follows: β-actin forward, 5-TCGTGCGTGACATCAAAGAG, and reverse, 5-TGGACAGT-GAGGCCAGGATG; mouse VASH1 forward, 5-GATTCCCATACCAAGTGT-GCC, and reverse, 5-ATGTGGCGGAAGTAGTTCCC (annealing temperature 62°C); mouse VASH2 forward, 5′-GGCTAAGCCTTCAATTCCCC, and reverse, 5′ CCCATTGGTGAGATAGATGCC (annealing temperature 64°C). Each mRNA level was measured as a fluorescent signal corrected according to the signal for β-actin.

Northern blot analysis

Northern blotting was performed as described.[11] Briefly, cells were starved in 0.1% FBS/αMEM. In some experiments, cells were stimulated with VEGF (Sigma-Aldrich) for 12 hours. Total RNA was then extracted by ISOGEN according to the manufacturer's instruction and was separated on a 1% agarose gel containing 2.2 M formaldehyde and transferred to a Hybond N^+ membrane. The membrane was hybridized with a ^{32}P-labeled VASH1 cDNA probe containing an open reading frame (464-1417). Autoradiography was performed on an imaging plate and analyzed with an FLA2000 (Fuji Film, Tokyo, Japan).

Intracellular localization of VASH1 and VASH2

To make a hemagglutinin (HA)–tagged construct, human VASH2 cDNA was cloned into the *Eco*R1-*Xho*1 site of internal ribosome entry site (IRES)–humanized Renilla green fluorescent protein (hrGFP) 2a vector (Stratagene, La Jolla, CA; VASH2, HA-IRES-GFP vector). To make GFP-fusion constructs, human VASH2 cDNA was cloned into CT-GFP TOPO vector (VASH2, CT-GFP vector) or NT-GFP TOPO vector (VASH2, NT-GFP vector; Invitrogen). Transfection was performed with Fugene 6 (Roche) according to the manufacturer's instructions. GFP-fusion protein was detected by the use of confocal microscopy.

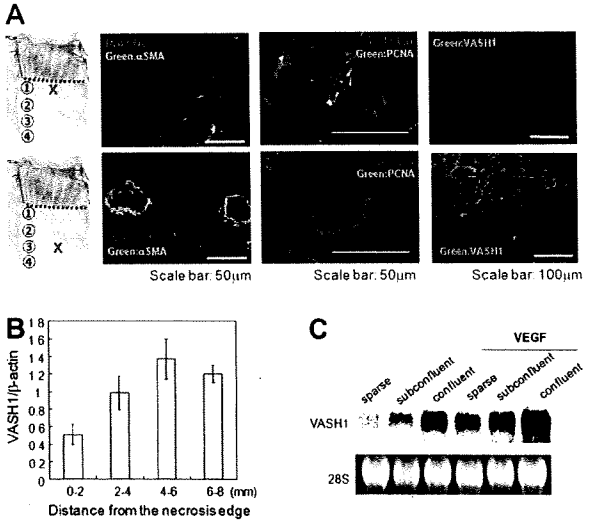

Figure 2. The spatiotemporal expression profile of VASH1. (A) Immunostaining of CD31 (red), αSMA (green), PCNA (green), and/or VASH1 (green) was performed with the indicated area of the skin flap. (B) Total RNA was isolated from each area of the skin flap. Quantitative real-time RT-PCR was performed to show mRNA levels of VASH1 in each area. Each value was standardized with β-actin. Data are expressed as mean and SDs. (C) HUVECs of sparse, subconfluent, and confluent conditions were treated with or without VEGF (1 nM) for 12 hours, and the expression of VASH1 was determined by Northern blotting.

Establishment of VASH1- or VASH2-expressing MS1 clones

To improve the activity of transcription, the CMV promoter of the pcDNA3.1/Hygro plasmid (Invitrogen) was replaced with the chicken β-actin promoter derived from pCALL2.[21] This vector, pCALL2-pcDNA3.1/Hygro, was used for the transfection in this study. Human VASH1 or VASH2 cDNA was cloned into the pCALL2-pcDNA3.1/Hygro vector at multiple cloning sites (*Xho*-I and *Not*-I). MS1 was transfected with the expression vector with the use of the Effectene transfection reagent (QIAGEN) according to the manufacturer's protocol. After the transfection, the cells were selected by hygromycin (500 μg/mL; Invitrogen).

Statistical analysis

The statistical significance of differences was evaluated by unpaired analysis of variances, and probability values were calculated with the Student *t* test. A value of P less than .05 was considered statistically significant.

Results

Mouse model of postnatal subcutaneous angiogenesis

To explore the roles of VASH family in the regulation of angiogenesis, we used a mouse model of postnatal subcutaneous angiogenesis. In this model, 2 parallel skin incisions were made on the back that penetrated the cutis, dermis, and underlying adipose tissue; a silicon sheet was inserted beneath the skin flap; and the incision was closed (Figure S1A, available on the *Blood* website; see the Supplemental Materials link at the top of the online article). The skin flap became hypoxic because the inserted silicon sheet blocked the blood supply from the deeper layer, and new vessels were distributed from the areas left undissected. Because of the substantial length of the skin incision, the central region became necrotic over the experimental period (Figure S1B). After 7 days, the skin flap was harvested and oriented parallel to the original incision for sectioning (Figure S2A). Pimonidazole staining showed that hypoxia was evident at the edge adjoining the necrotic tissue (Figure S2B).

We evaluated the skin flap at every 2-mm interval from the necrotic edge and determined the vessel distribution in each area (Figure 1A). In this way, the entire progress of angiogenesis could be observed from a single section. The area 0 to 4 mm from the necrotic edge contained mostly small vessels with PCNA-positive proliferating ECs (Figure 1A). This area was thus defined as the sprouting front of angiogenesis. The elevation of vascular luminal area and vascular numbers was most prevalent in the area 2 to 4 mm from the necrotic edge (Figure 1B). The area further than 4 mm from the necrotic edge contained hierarchical vasculature of small and large vessels with PCNA-negative nonproliferating ECs surrounded by αSMA-positive mural cells (Figure 1A). This area was thus defined as the termination zone of angiogenesis. Vascular luminal area and vascular numbers were decreased in this area (Figure 1B).

Spatiotemporal expression profile of VASH1 and VASH2 during angiogenesis

During the postnatal period, the expression of VASH1 and VASH2 proteins is only faintly shown in arterial ECs under the basal condition.[16] Here, we determined VASH2 mRNA in various organs

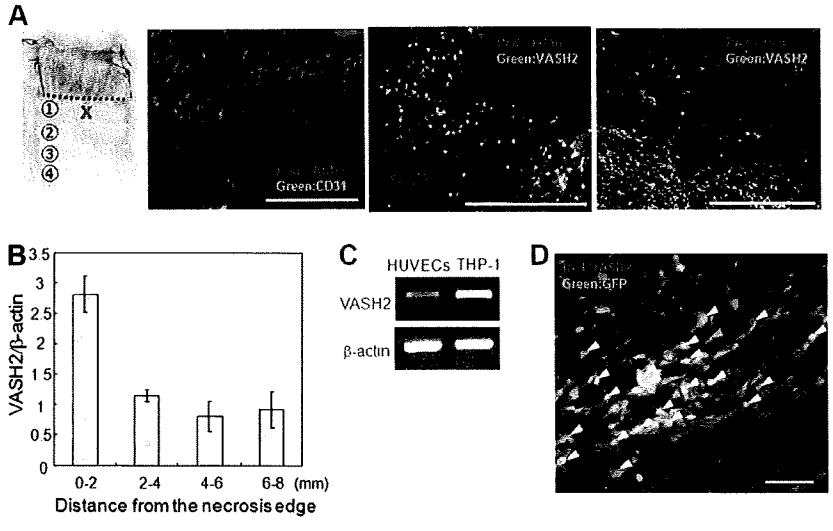

Figure 3. The spatiotemporal expression profile of VASH2. (A) Immunostaining of VASH2, CD11b, and F4/80 in the area 0 to 2 mm from the necrotic edge. Scale bars are 200 μm. (B) Total RNA was isolated from each area of the skin flap. Quantitative real-time RT-PCR was performed to show mRNA levels of VASH2 in each area. Each value was standardized with β-actin. (C) The basal level of VASH2 mRNA in HUVECs or THP-1 cells was determined by RT-PCR. (D) After confirming bone marrow reconstitution, the subcutaneous angiogenesis experiment was performed. Immunostaining of VASH2 in the area 0 to 2 mm from the necrotic edge is shown. Arrowheads indicate GFP-positive and VASH2-positive cells. Scale bar is 50 μm.

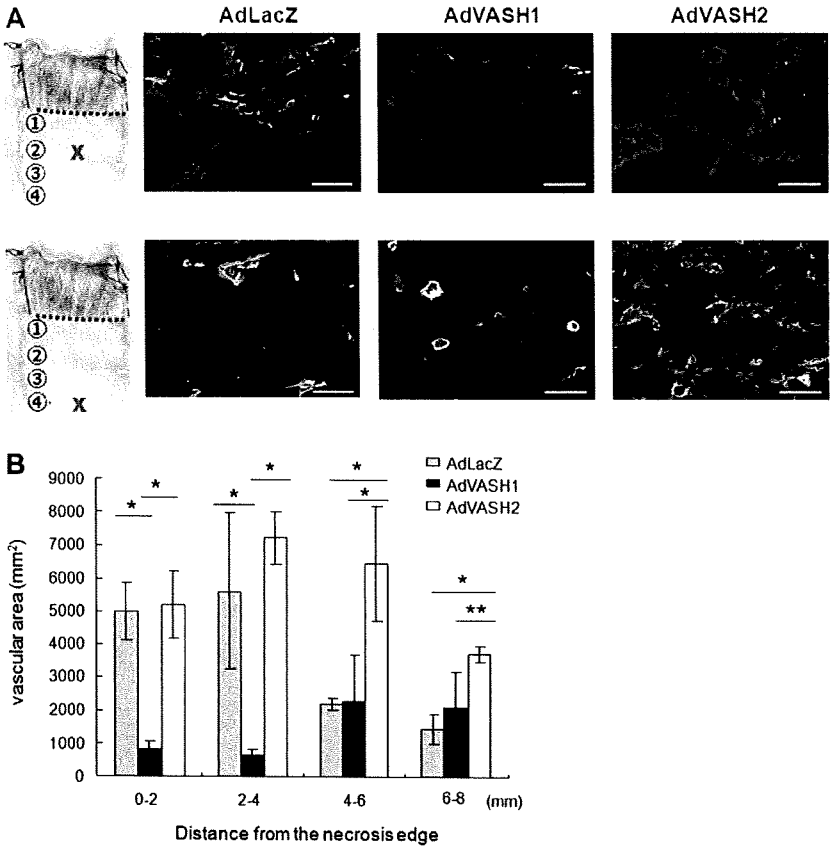

Figure 4. Effects of exogenous VASH1 or VASH2 on angiogenesis in the skin flap. AdVASH1 or AdVASH2 was injected into the tail vein to supply sufficient exogenous proteins to the site of angiogenesis. (A) Immunostaining of CD31 (red) and αSMA (green) positive cells in the indicated area of the skin flap. Scale bars are 50 μm. (B) Vascular area was determined from 5 different fields in each area. Data are expressed as the means and SDs; $^{*}P < .01$, $^{**}P < .05$.

in mice (Figure S3). This restricted expression pattern of VASH2 was comparable with that of VASH1,[11] and it further confirmed that basal expression of these 2 proteins is quite low. However, we have already reported that VASH1 is selectively present in ECs at the site of angiogenesis.[11,14,15]

Here, we determined their expression during angiogenesis more precisely. Immunostaining of VASH1 protein showed that PCNA-positive ECs in small vessels at the sprouting front were faintly stained, whereas PCNA-negative ECs surrounded by mural cells in the termination zone were intensely stained (Figure 2A). Quantitative real-time RT-PCR further confirmed that VASH1 mRNA was lowest in the area 0 to 2 mm from the necrotic edge, increased and was most prevalent in the area of 4 to 6 mm from the necrotic edge, and then declined thereafter (Figure 2B). Because VASH1 was identified as a VEFG-inducible molecule,[11] we initially thought that ECs in the sprouting front expressed VASH1 abundantly. However, it was not the case. We therefore reevaluated the expression pattern of VASH1 by using cultured HUVECs. What we found was that the expression level of VASH1 was dependent on the culture conditions. The basal expression of VASH1 in exponentially proliferating HUVECs was extremely low, increased in subconfluent to confluent cultures, although VEGF-inducibility was maintained (Figure 2C). Thus, the expression profile of VASH1 in the skin flap correlated with what we found in the culture condition.

We then determined the expression of VASH2 in this system. We noted that VASH2 protein was preferentially localized in infiltrating MNCs in the area 0 to 2 mm from the necrotic edge (Figure 3A). These MNCs were CD11b-positive but F4/80-negative (Figure 3A). Although we showed the specificity of our antibodies previously,[16] the specificity was further confirmed, because VASH1 was negative in MNCs in the sprouting front (Figure 2A), whereas VASH2 was negligible in ECs in the termination zone (Figure S4). Quantitative real-time RT-PCR further confirmed that VASH2 mRNA was highest in the area 0 to 2 mm from the necrotic edge (Figure 3B). We could also show that monocytic TPH-1 cells expressed VASH2 mRNA more abundantly than HUVECs (Figure 3C).

It has been well accepted that bone marrow–derived cells contribute to angiogenesis.[22] We therefore hypothesized that these MNCs were derived from bone marrow. To prove this, we lethally irradiated wild-type mice and transplanted them with bone marrow cells from mice ubiquitously expressing green fluorescent protein (GFP-mice). After confirming bone marrow reconstitution, we performed the subcutaneous angiogenesis analysis. We observed that most of the VASH2-positive MNCs were positive for GFP (Figure 3D arrowheads). We could hardly detect GFP-positive cells integrated in the wall of neo-vessels.

These results indicate that VASH1 is expressed by ECs in the termination zone, whereas VASH2 is mainly expressed by bone marrow–derived MNCs infiltrating the sprouting front.

Effects of exogenous VASH1 or VASH2 on angiogenesis

To evaluate the effect of exogenous VASH1 or VASH2, we injected AdVASH1 or AdVASH2 into the tail vein of mice to cause expression of these genes in the liver. We confirmed the expression of VASH1 or VASH2 in the liver (data not shown). As described previously, this procedure supplied sufficient proteins to regulate angiogenesis in the remote site.[15] Adenovirus-mediated transfer of the *VASH1* gene inhibited angiogenesis at the sprouting front where endogenous VASH1 was scarce, but it did not influence vascularity in the termination zone where endogenous VASH1 was enriched (Figure 4A,B). Adenoviral-mediated transfer of the *VASH2* gene

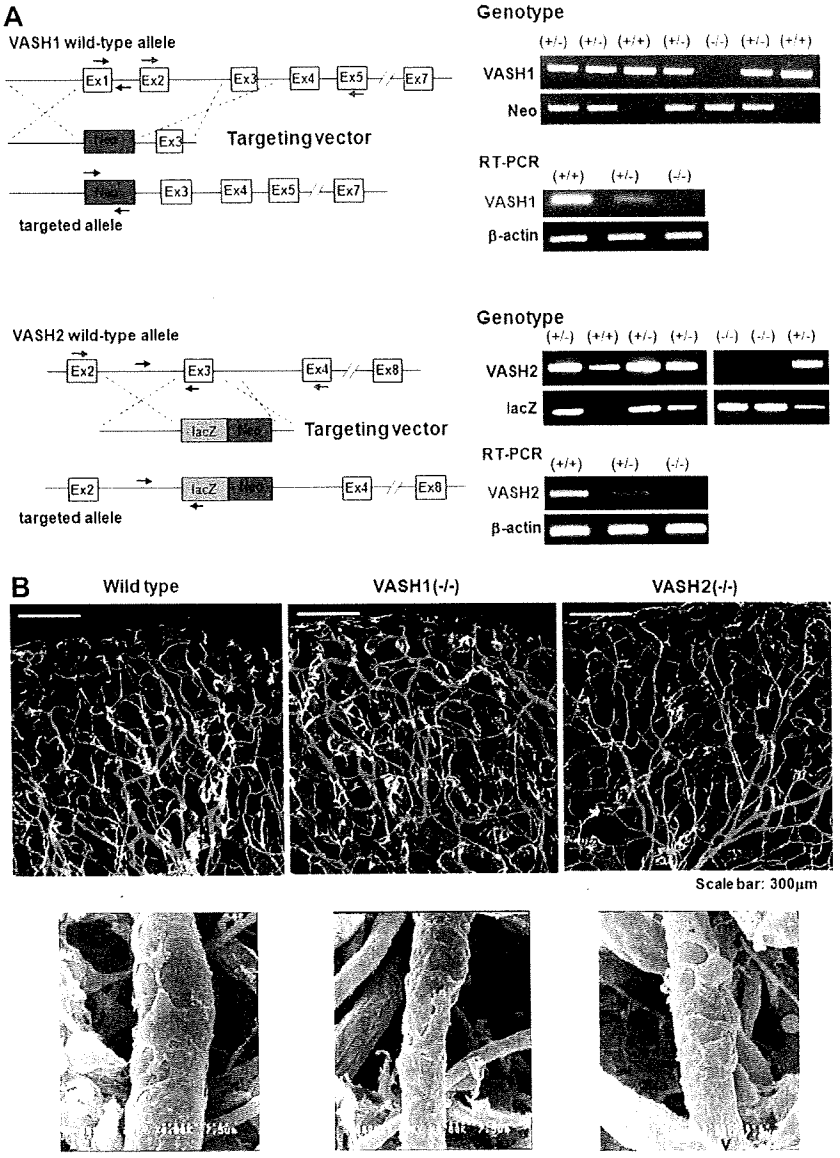

Figure 5. Generation of *VASH1* and *VASH2* knockout mice and their steady state subcutaneous vascular architecture. (A) *VASH1* and *VASH2* knockout mice were generated as described in "Generation of VASH1 and VASH2 knockout mice." Genotyping and the analysis of each transcript by RT-PCR are shown. (B) Ear skin was used to show the steady state vascular architecture of ear skin. Top panels show immunostaining of CD31 (green) and LYVE-1 (red). Bottom panels show SEM of capillary vessels.

did not cause any changes in the sprouting front, but it sustained the increased vascularity in the termination zone (Figure 4A,B). These opposing effects of VASH1 and VASH2 were further confirmed in vitro by the stable transfection of the *VASH1* or *VASH2* gene into cultured ECs (Figure S5). Both VASH1 and VASH2 lack classical signal sequences.[11,16] We have previously shown that VASH1 is an endoplasmic reticulum–independent secretory protein. To compare the intracellular localization of VAS1 and VASH2 proteins, we constructed the GFP-fused human *VASH2* expression vectors and transfected them into GM7373 cells. We simultaneously transfected human *VASH1* gene with the use of AdVASH1. As shown in Figure S6, the intracellular localization of VASH1 and VASH2 was comparable. In consequence, exogenous VASH1 inhibits angiogenesis at the sprouting front, whereas exogenous VASH2 prolongs angiogenesis in the termination zone.

Function of endogenous VASH1 or VASH2 on angiogenesis

To further clarify the function of endogenous VASH1 and VASH2, we generated *VASH1* or *VASH2* knockout mice by conventional homologous recombination (Figure 5A). We examined the steady state vascular architecture of ear subcutis of survived mice. We could not find any significant changes of vascular architecture in either *VASH1* knockout or *VASH2* knockout mice (Figure 5B).

We then subjected the *VASH1* knockout and *VASH2* knockout mice to the model of subcutaneous angiogenesis. The degree of vascular area at the sprouting front was almost identical between wild-type, *VASH1*$^{+/-}$, and *VASH1*$^{-/-}$ mice (Figure 6B). The vascular area significantly decreased in the termination zone in the wild-type mice where endogenous VASH1 was enriched, but that was maintained in higher degree in *VASH1* knockout mice (Figure 6A). Quantitative analysis showed that this change was gene-dosage sensitive (Figure 6B). Lectin staining indicated that new vessels of *VASH1*$^{-/-}$ mice were patent and maintained blood flow (Figure 6C). Supplementation of the deficient proteins by adenoviral-mediated gene transfer normalized the abnormal angiogenesis patterns in *VASH1* knockout (Figure 6D).

In contrast, the vascular density was lower in entire areas in the *VASH2* knockout mice (Figure 7B). This change was gene-dosage

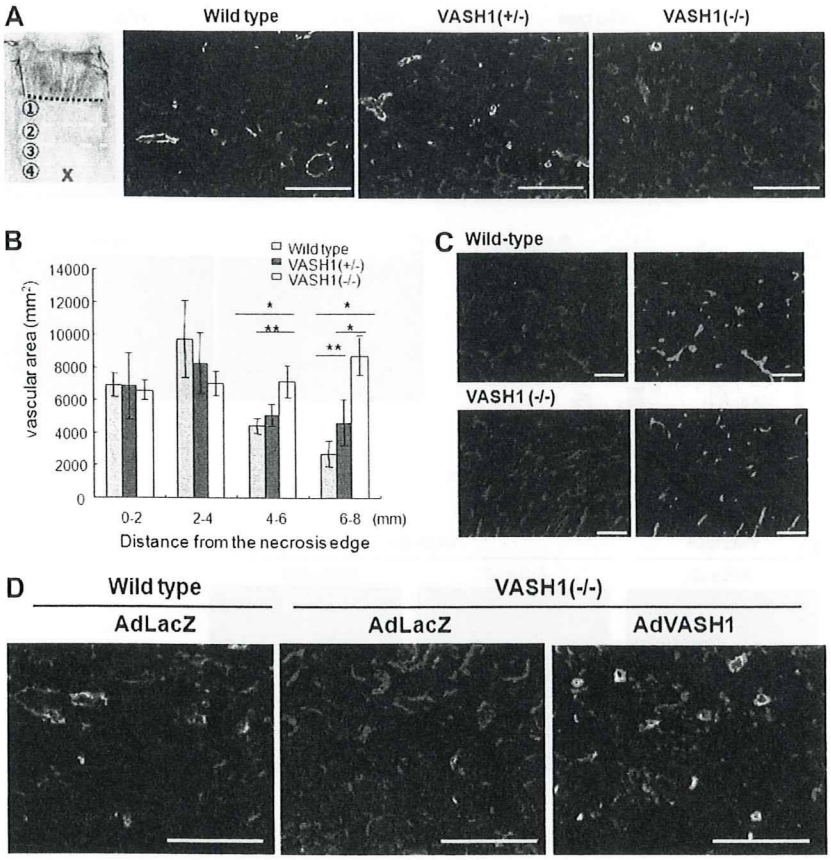

Figure 6. Vascular distribution in the skin flap of *VASH1* knockout mice. *VASH1* knockout mice were applied to the model of subcutaneous angiogenesis. (A) Immunostaining of CD31 (red) and αSMA (green) in the area 6 to 8 mm from the necrotic edge is shown. Scale bars are 200 μm. (B) The vascular area was determined from 5 different fields in each area. Data are expressed as the means and SDs; $^{*}P < .01$, $^{**}P < .05$. (C) Lectin staining (green) shows the perfusion of new vessels in the area 6 to 8 mm from the necrotic edge. The same section was immunostained for CD31 (red). Scale bars are 200 μm. (D) Adenoviral-mediated gene transfer was performed to supplement the deficient protein in *VASH1* knockout mice. AdLacZ was use as the control. Immunostaining of CD31 (red) and αSMA (green) in the indicated area of the skin flap is shown. Scale bars are 200 μm.

sensitive at the sprouting front where endogenous VASH2 should be enriched (Figure 7A,B). Importantly, the extent of MNC infiltration in the sprouting front was not altered in *VASH2*$^{-/-}$ mice (Figure 7C). Again, supplementation of the deficient proteins by adenoviral-mediated gene transfer normalized the abnormal angiogenesis patterns in *VASH2* knockout mice (Figure 7D).

Discussion

We characterized the roles of the 2 members of the vasohibin family in the regulation of angiogenesis with the use of a mouse model of subcutaneous angiogenesis. The spatiotemporal expression pattern and substantial effects of these 2 molecules indicate that VASH1 and VASH2 control the promotion and termination of angiogenesis in a complementary manner.

The expression of endogenous VASH1 was augmented in nonproliferating ECs in the termination zone of postnatal angiogenesis. This VASH1 in the termination zone should be involved in halting angiogenesis, because angiogenesis persisted in the termination zone in *VASH1* knockout mice in a gene-dosage manner. This result also implies that endogenous VASH1 is not a principal regulator limiting the sprouting. However, when applied exogenously, VASH1 can inhibit angiogenesis at the sprouting front where endogenous VASH1 is scarce. In addition, exogenous VASH1 exhibits little effect, if any, in the termination zone where endogenous VASH1 is present. Accordingly, the present results show the distinctive acting points of endogenous and exogenous VASH1 and further support the legitimacy of using exogenous VASH1 as an antiangiogenic treatment.

Endogenous VASH2, in contrast, was expressed mainly by infiltrating bone marrow–derived MNCs at the sprouting front in our model. The present result contrasts with our previous observation about VASH2 expression in ECs of developing embryos without obvious MNC infiltration.[16] About the expression of VASH2 in MNCs, monocytic THP-1 cells were found to express VASH2 more abundantly than ECs in culture. Hence, MNCs can be the main source of VASH2 when they infiltrate.

Bone marrow–derived cells, including endothelial progenitor cells (EPCs), contribute to postnatal angiogenesis.[22] However, we could hardly detect the integration of bone marrow–derived cells in the neo-vessels in our model, indicating that EPCs might not play a major role in our model. What we observed was that most of the bone marrow–derived cells infiltrated in the sprouting front were MNCs. It is described that bone marrow–derived MNCs stimulate angiogenesis by producing angiogenic factors, including VEGF and several matrix metalloproteinases.[23,24] Along these lines, we propose that VASH2 produced by bone marrow–derived MNCs takes part in the promotion of postnatal angiogenesis, because angiogenesis at the sprouting front is significantly impaired in *VASH2* knockout mice even in the presence of MNC infiltration. Appropriately, exogenous VASH2 inhibited the termination of angiogenesis in the termination zone where endogenous VASH2 staining was faint.

We previously reported that, when applied exogenously, VASH-2 exhibited the antiangiogenic activity in the mouse cornea.[16] However, to our surprise, the present study rather indicated the proangiogenic activity of VASH2. Amino acid sequence of VASH2 is 52.5% homologous to that of VASH1 in humans, and 51.9% homologous in mice.[16] We therefore hypothesize the role of

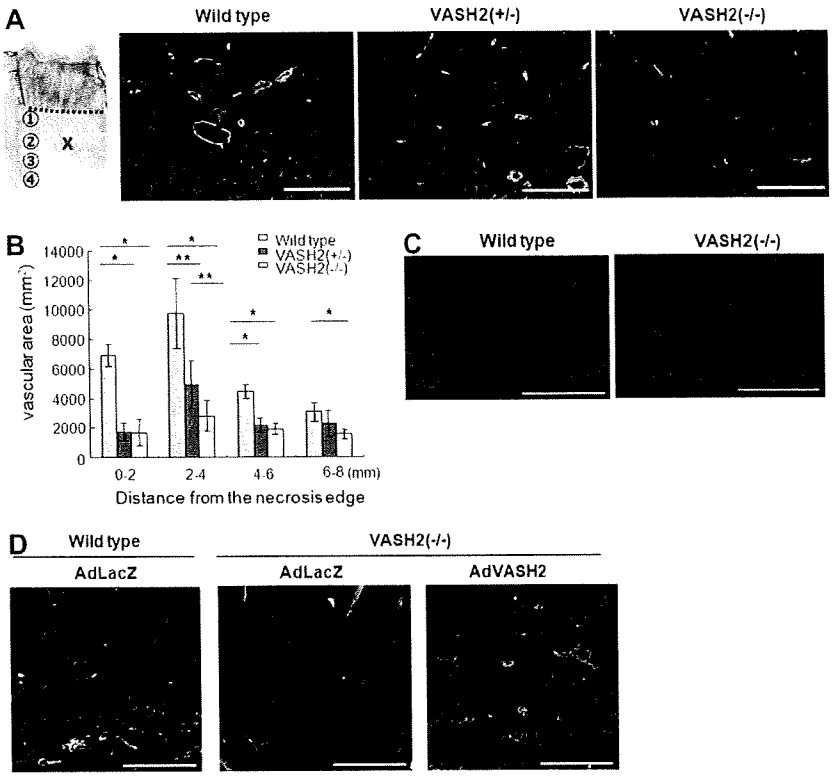

Figure 7. Vascular distribution in the skin flap of *VASH2* knockout mice. *VASH2* knockout mice were applied to the model of subcutaneous angiogenesis. (A) Immunostaining of CD31 (red) and αSMA (green) in the area 2 to 4 mm from the necrotic edge is shown. Scale bars are 200 μm. (B) The vascular area was determined from 5 different fields in each area. Data are expressed as the means and SDs; $^{*}P < .01$, $^{**}P < .05$. (C) Immunostaining of CD11b (red) in the area 0 to 2 mm from the necrotic edge is shown in wild-type and *VASH2*$^{-/-}$ mice. Scale bars are 200 μm. (D) Adenoviral-mediated gene transfer was performed to supplement the deficient protein in *VASH2* knockout mice. AdLacZ was use as the control. Immunostaining of CD31 (red) and αSMA (green) in the indicated area of the skin flap is shown. Scale bars are 200 μm.

VASH2 as follows. On the analogy to angiopoietin-1 and angiopoietin-2, VASH1 and VASH2 may share the same receptor. VASH2 is a weak agonist and antagonizes VASH1 in a certain condition, although the receptor for the VASH family is not yet identified. We are currently testing this hypothesis.

There are several endogenous angiogenesis inhibitors in the body, but it is still not clear why the body needs so many angiogenesis inhibitors. Systematic analysis to show how these endogenous angiogenesis inhibitors orchestrate the control of angiogenesis is lacking. Delta-like 4 (Dll4) is the ligand of Notch1, which determines the arterial specification of ECs.[25,26] However, recent evidence indicates that ECs at the sprouting tip express Dll4 and that this Dll4 negatively regulates the formation of appropriate numbers of sprouting tips.[27-31] Therefore, Dll4 and VASH1 are 2 inhibitors that are expressed in ECs, but the apparent difference between VASH1 and Dll4 is their temporal expression patterns. Dll4 is selectively expressed in tip cells, whereas VASH1 is expressed in ECs in the termination zone. Hence, VASH1 and Dll4 are expressed in different phases of angiogenesis and should negatively tune this phenomenon distinctively. It is described that inactivation of Dll4 increases sprouting microvessels without proper blood perfusion.[32,33] Importantly, increased numbers of microvessels in the termination zone of *VASH1*$^{-/-}$ mice were patent and maintained blood perfusion. This difference in blood perfusion further proposes the distinctive roles of VASH1 and Dll4 in the regulation of angiogenesis.

In summary, the vasohibin family members, VASH1 and VASH2, participate in the regulation of angiogenesis in a previously unrecognized manner. VASH1 is expressed in ECs in the termination zone to halt angiogenesis, whereas VASH2 is expressed mainly in infiltrating MNCs at the sprouting front to promote angiogenesis. Discovery of these molecules should provide novel approaches to both antiangiogenic and proangiogenic treatments. Further study is currently under way to clarify the underlying mechanism how VASH1 and VASH2 regulate angiogenesis in an opposed but complementary manner.

Acknowledgments

This work was supported by a Grant-in-Aid for Scientific Research on Priority Areas of the Japanese Ministry of Education, Science, Sports, and Culture from the Ministry of Education, Science, Sports, and Culture of Japan (contract grants 16022205 and 17014006), and by the 21st Century COE Program Special Research Grant "The Center for Innovative Therapeutic Development Towards the Conquest of Signal Transduction Diseases" from the Ministry of Education, Science, Sports, and Culture of Japan.

Authorship

Contribution: H.K. performed research and wrote the paper; H.M. and Y.S. prepared the knockout mice; M.K. performed transfection to MS1 cells; K.W. performed analysis of the intracellular localization; H.S. and H.O. prepared antibodies; T.F. performed electron microscopy; T.S. designed the research; and Y.S. designed the research and wrote the paper.

Conflict-of-interest disclosure: The authors declare no competing financial interests.

Correspondence: Yasufumi Sato, Department of Vascular Biology, Institute of Development, Aging and Cancer, Tohoku University, 4-1 Seiryo-machi, Aoba-ku, Sendai 980-8575, Japan; e-mail: y-sato@idac.tohoku.ac.jp.

References

1. Adams RH, Alitalo K. Molecular regulation of angiogenesis and lymphangiogenesis. Nat Rev Mol Cell Biol. 2007;8:464-478.
2. Sato Y. Update on endogenous inhibitors of angiogenesis. Endothelium. 2006;13:147-155.
3. Dawson DW, Volpert OV, Gillis P, Crawford SE, et al. Pigment epithelium-derived factor: a potent inhibitor of angiogenesis. Science. 1999;285:245-248.
4. Renno RZ, Youssri AI, Michaud N, Gragoudas ES, Miller JW. Expression of pigment epithelium-derived factor in experimental choroidal neovascularization. Invest Ophthalmol Vis Sci. 2002;43:1574-1580.
5. Hiraki Y, Inoue H, Iyama K, et al. Identification of chondromodulin I as a novel endothelial cell growth inhibitor. Purification and its localization in the avascular zone of epiphyseal cartilage. J Biol Chem. 1997;272:32419-32426.
6. Yoshioka M, Yuasa S, Matsumura K, et al. Chondromodulin-I maintains cardiac valvular function by preventing angiogenesis. Nat Med. 2006;12:1151-1159.
7. Zhang M, Volpert O, Shi YH, Bouck N. Maspin is an angiogenesis inhibitor. Nat Med. 2000;6:196-199.
8. Maass N, Nagasaki K, Ziebart M, Mundhenke C, Jonat W. Expression and regulation of tumor suppressor gene maspin in breast cancer. Clin. Breast Cancer. 2002;3:281-287.
9. Kopp HG, Hooper AT, Broekman MJ, et al. Thrombospondins deployed by thrombopoietic cells determine angiogenic switch and extent of revascularization. J Clin Invest. 2006;116:3277-3291.
10. Kalluri R. Basement membranes: structure, assembly and role in tumour angiogenesis. Nat Rev Cancer. 2003;3:422-433.
11. Watanabe K, Hasegawa Y, Yamashita H, et al. Vasohibin as an endothelium-derived negative feedback regulator of angiogenesis. J Clin Invest. 2004;114:884-886.
12. Shimizu K, Watanabe K, Yamashita H, et al. Gene regulation of a novel angiogenesis inhibitor, vasohibin, in endothelial cells. Biochem Biophys Res Commun. 2005;327:700-7006.
13. Sonoda H, Ohta H, Watanabe K, Yamashita H, Kimura H, Sato Y. Multiple processing forms and their biological activities of a novel angiogenesis inhibitor vasohibin. Biochem Biophys Res Commun. 2006;342:640-646.
14. Shen JK, Yang XR, Sato Y, Campochiaro PA. Vasohibin is up-regulated by VEGF in the retina and suppresses VEGF receptor 2 and retinal neovascularization. FASEB J. 2006;20:723-725.
15. Yamashita H, Abe M, Watanabe K, et al. Vasohibin prevents arterial neointimal formation through angiogenesis inhibition. Biochem Biophys Res Commun. 2006;345:919-925.
16. Shibuya T, Watanabe K, Yamashita H, et al. Isolation of vasohibin-2 as a sole homologue of VEGF-inducible endothelium-derived angiogenesis inhibitor vasohibin: a comparative study on their expressions. Arterioscler Thromb Vasc Biol. 2006;26:1051-1057.
17. Sato Y, Sonoda H. The vasohibin family: a negative regulatory system of angiogenesis genetically programmed in endothelial cells. Arterioscler Thromb Vasc Biol. 2007;27:37-41.
18. Tepper OM, Capla JM, Galiano RD, et al. Adult vasculogenesis occurs through in situ recruitment, proliferation, and tubulization of circulating bone marrow-derived cells. Blood. 2005;105:1068-1077.
19. Oike Y, Akao M, Yasunaga K, et al. Angiopoietin-related growth factor antagonizes obesity and insulin resistance. Nat Med. 2005;11:400-408.
20. Yamazaki D, Suetsugu S, Miki H, et al. WAVE2 is required for directed cell migration and cardiovascular development. Nature. 2003;424:452-456.
21. Namba K, Abe M, Saito S, et al. Indispensable role of the transcription factor PEBP2/CBF in angiogenic activity of a murine endothelial cell MSS31. Oncogene. 2000;19:106-114.
22. Rabbany SY, Heissig B, Hattori K, Rafii S. Molecular pathways regulating mobilization of marrow-derived stem cells for tissue revascularization. Trends Mol Med. 2003;9:109-117.
23. Barbera-Guillem E, Nyhus JK, Wolford CC, Friece CR, Sampsel JW. Vascular endothelial growth factor secretion by tumor-infiltrating macrophages essentially supports tumor angiogenesis, and IgG immune complexes potentiate the process. Cancer Res. 2002;62:7042-7049.
24. Cho CH, Koh YJ, Han J, et al. Angiogenic role of LYVE-1-positive macrophages in adipose tissue. Circ Res. 2007;100:e47-57.
25. Shutter JR, Scully S, Fan W, et al. Dll4, a novel Notch ligand expressed in arterial endothelium. Genes Dev. 2000;14:1313-1318.
26. Duarte A, Hirashima M, Benedito R, et al. Dosage-sensitive requirement for mouse Dll4 in artery development. Genes Dev. 2004;18:2474-2478.
27. Williams CK, Li JL, Murga M, Harris AL, Tosato G. Up-regulation of the Notch ligand Delta-like 4 inhibits VEGF-induced endothelial cell function. Blood. 2006;107:931-939.
28. Hellstrom M, Phng LK, Hofmann JJ, et al. Dll4 signalling through Notch1 regulates formation of tip cells during angiogenesis. Nature. 2007;445:776-780.
29. Siekmann AF, Lawson ND. Notch signalling limits angiogenic cell behaviour in developing zebrafish arteries. Nature. 2007;445:781-784.
30. Leslie JD, Ariza-McNaughton L, Bermange AL, McAdow R, Johnson SL, Lewis J. Endothelial signaling by the Notch ligand Delta-like 4 restricts angiogenesis. Development. 2007;134:839-844.
31. Lobov IB, Renard RA, Papadopoulos NJ, et al. Delta-like ligand 4 (Dll4) is induced by VEGF as a negative regulator of angiogenic sprouting. Proc Natl Acad Sci U S A. 2007;104:3219-3224.
32. Noguera-Troise I, Daly C, Papadopoulos NJ, et al. Blockade of Dll4 inhibits tumour growth by promoting nonproductive angiogenesis. Nature. 2006;444:1032-1037.
33. Ridgway J, Zhang G, Wu Y, et al. Inhibition of Dll4 signalling inhibits tumour growth by deregulating angiogenesis. Nature. 2006;444:1083-1087.

J. Biochem. 2009;145(5)653–659
doi:10.1093/jb/mvp021

Induction and Expression of Anti-Angiogenic Vasohibins in the Hematopoietic Stem/Progenitor Cell Population

Hisamichi Naito[1], Hiroyasu Kidoya[1], Yasufumi Sato[2] and Nobuyuki Takakura[1,*]

[1]Department of Signal Transduction, Research Institute for Microbial Diseases, Osaka University, 3-1 Yamada-oka, Suita-shi, Osaka 565-0871, Japan; and [2]Department of Vascular Biology, Institute of Development, Aging, and Cancer, Tohoku University, 4-1 Seiryo-machi, Aoba-ku, Sendai 980-8575, Japan

Received January 8, 2009; accepted January 23, 2009; published online January 29, 2009

Haematopoiesis and blood vessel formation are closely associated, with several molecules employed by both systems. Recently, vasohibin-1 (VASH1), an endothelium-derived negative feedback regulator of angiogenesis, has been isolated and characterized. VASH1 is induced by VEGF or bFGF in endothelial cells (ECs) and inhibits their proliferation and migration. However, there are no data on the induction and expression of VASH1 in haematopoietic cells (HCs). Here, we show that the haematopoietic stem cell (HSC) population, but not haematopoietic progenitors (HPs) or mature HCs from adult bone marrow (BM) constitutively express VASH1. However, HPs, but not HSCs, can be induced to express VASH1 after BM suppression by 5-FU. Knock-down of the *VASH1* gene in VASH1$^+$ leukaemia cells induced cell proliferation. These results suggest a role for VASH1 in negative feedback regulation of HP proliferation during recovery following BM ablation.

Key words: 5-FU, bone marrow ablation, haematopoietic progenitor cells, haematopoietic stem cell, vasohibin.

Abbreviations: bFGF, basic fibroblast growth factor; BM, bone marrow; EC, endothelial cell; HC, haematopoietic cell; HP, haematopoietic progenitor; HSC, haematopoietic stem cell; VASH1, vasohibin-1; VEGF, vascular endothelial growth factor.

The haematopoietic and vascular systems are closely related in several respects. It has been suggested that haematopoietic cells (HCs) and endothelial cells (ECs) arise from a common progenitor during development, the so-called haemangioblast (*1*) or hemogenic angioblast (*2*), which originates from mesodermal cells. In addition, after the development of haematopoietic stem cells (HSCs) and ECs, the latter supports the differentiation, proliferation and survival of the former, which themselves support angiogenesis (*3–10*). Moreover, it has been reported that erythropoietin, originally identified as a haematopoietic cytokine, also induces proliferation of ECs (*11*), suggesting that there are several factors commonly utilized in vascular development and haematopoiesis.

Recently, a novel anti-angiogenic factor, vasohibin-1 (VASH1), has been isolated from human umbilical vein endothelial cells (HUVECs) (*12*). VASH1 is upregulated by vascular endothelial growth factor (VEGF) in HUVECs and has been suggested to act as a negative feedback regulator of VEGF and basic fibroblast growth factor (bFGF) signalling in HUVECs. VASH1 is widely conserved among species (*13*) and is present in multiple processing forms (*14*), and it has been reported that alternative splicing of the VASH1 pre-mRNA transcript generates a potent anti-angiogenic protein (*15*). However, in mice, alternatively spliced forms of VASH1 have not been isolated. One VASH1 paralogue, termed vasohibin-2 (VASH2), with anti-angiogenic activity in mammals, has also been isolated recently (*16*). VASH1 is upregulated in retina upon stimulation with VEGF and suppresses retinal neovascularization in mice with ischemic retinopathy (*17*). VASH1 expression has been observed in ECs of adventitial microvessels in atherosclerotic lesions, where it inhibits adventitial angiogenesis and neointimal formation after cuff placement on the mouse femoral artery (*18*). Moreover, VASH1 is selectively expressed on vascular EC in both cyclic endometria and endometrial carcinomas and suppresses tumour growth and angiogenesis in a mouse xenograft tumour model (*19*). Taken together, these data suggest that VASH1 is a candidate target molecule for manipulating tumour angiogenesis.

While the unique function of VASH1 as a negative feedback regulator of angiogenesis has been extensively studied, its expression in cell lineages other than ECs has not been documented. On the basis of the hypothesis that the haematopoietic and vascular systems utilize similar molecules, here, we investigated the expression of VASH1 in several fractions of normal HCs in the bone marrow (BM) as well as in leukaemic cells and assessed the mechanisms regulating HC VASH1 expression.

MATERIALS AND METHODS

Mice—C57BL/6 mice were purchased from SLC (Shizuoka, Japan). All animal studies were approved by

*To whom correspondence should be addressed. Tel: +81-6-6879-8316, Fax: +81-6-6879-8314,
E-mail: ntakaku@biken.osaka-u.ac.jp

the Animal Care Committee of Osaka University. For BM ablation studies, 10-week-old mice were treated with a single-tail vein injection of 5-FU (Kyowa Hakko Kogyo Co., Ltd, Tokyo, Japan; 150 mg/kg body weight). The mouse model of hind limb ischemia was as described previously (*3*).

Cell Preparation and Flow Cytometry—Cell preparation from the hind limb, BM and peripheral blood was carried out as previously reported (*3*). The cell-staining procedure for flow cytometry was as described previously (*3*) using anti-CD31, -CD45, -c-kit, -Sca-1 and anti-lineage (a mixture of ter119, Gr-1, Mac-1, B220, CD4 and CD8) monoclonal antibodies (mAbs; all from Pharmingen). All mAbs were purified and conjugated with either FITC or PE (phycoerythrin) or biotin. Biotinylated antibodies were visualized with PE-conjugated streptavidin or APC-conjugated streptavidin (Pharmingen). The stained cells were analysed and sorted by JSAN (Bay Bioscience, Kobe, Japan). For the procedures involving SP cells, Hoechst dye was used as previously described (*20*, *21*). BMMNCs were resuspended at 1×10^6 cells/ml and incubated with Hoechst 33342 (5 μg/ml) for 90 min at 37°C. Cells were then washed and analysed by JSAN (Bay Bioscience).

Quantitative Real-Time Reverse Transcription PCR (qRT-PCR) Analysis—Extraction of total RNA and qRT–PCR was performed as previously reported (*22*). Levels of specific amplified cDNA were normalized to *glyceraldehyde-3-phosphate dehydrogenase* (*GAPDH*) housekeeping gene levels. Primers used in this experiment were as follows: mouse *VASH1* (corresponding to human *VASH1A*, sense 5′-CAT CAG GGA GCT GCA GTA CA-3′, anti-sense 5′-GAT CAC AGC TTC CAG GCA TT-3′), human *VASH1A* (sense 5′-GCT GCA GTA CAA TCA CAC AGG-3′, anti-sense 5′-AGG TAA ATT CCC AGG ATC ACG-3′), human *VASH1B* (sense 5′-AAG CTG TGC AGC GTC ACA TC-3′, anti-sense 5′-ACT TTC AGA GCA GGA AGC TGA-3′) (*15*), mouse *GAPDH* (sense 5′-TGG CAA AGT GGA GAT TGT TGC C-3′, anti-sense 5′-AAG ATG GTG ATG GGC TTC CCG-3′), human *GAPDH* (sense 5′-GAA GGT GAA GGT CGG AGT C-3′ and anti-sense 5′-GAA GAT GGT GAT GGG ATT TC-3′).

Western Blotting Analysis—Methods for western blotting were previously described (*22*). Antibodies used in this experiment were anti-VASH1 (*12*) and anti-GAPDH (Chemicon, Temecula, CA).

Cell Lines—HUVECs were purchased from Kurabo (Osaka, Japan) and cultured in Humedia EG2 (Kurabo). For the induction analysis of VASH1A, HUVECs were starved for 12 h and stimulated with VEGF-A_{165} (10 ng/ml, PeproTech, Rocky Hill, NJ) for 12 h.

Human leukaemia cell lines (KG1a, HL60, THP-1, MOLT-4, SKW3, BALL-1 and NALM6) as indicated in Fig. 4A were provided by the Riken Bioresource Center (Tsukuba, Japan) and the Cell Resource Center for Biomedical Research, Institute of Development, Aging and Cancer, Tohoku University.

RNAi and Transfection—Two Stealth™ RNAi duplexes were synthesized commercially by Invitrogen. Stealth RNAi duplexes with GC content similar to that of each test duplex were used as a negative control. Stealth™ RNAi #1 (5′-UCU GAU AUA GCG CUG CAC AGC UUC C-3′), Stealth™ RNAi #2 and Stealth™ RNAi #2 (5′-UUC CCU GAG AAG UAG GUC UUG AAG C-3′) were designed to target different coding regions of the human *Vash1* mRNA sequence. A BLAST (NCBI database) search was carried out to confirm that the targets of the two Stealth™ RNAi duplexes were exclusively in *Vash1*.

THP1 cells were seeded at 1×10^5 cells/ml, and transfection was accomplished using lipofectamine 2000 according to the manufacturer's instructions. For selecting transfected cells, each Stealth RNAi duplex was co-transfected with Block-iT Alexa Fluor Red Flurescent Oligo (Invitrogen) and 24 h later, positive cells were sorted by JSAN (Bay Bioscience) and cultured for growth assessment.

Statistical Analysis—All data are presented as mean ± SD. For statistical analysis, the statcel2 software package (OMS) was used with analysis of variance (ANOVA) performed on all data followed by Tukey–Kramer multiple comparison testing.

RESULTS

Expression of VASH1 in the HSC Population of Adult BM—Adult bone marrow (BM) cells were fractionated into a $Lin^-c\text{-}Kit^+Sca\text{-}1^+$ HSC-enriched population (KSL cells), a Lin^- haematopoietic progenitor (HP)-enriched population (Lin^- cells) and a differentiated HC (Lin^+ cells) population (Fig. 1A). qRT–PCR analysis (Fig. 1C) indicated that KSL cells express *VASH1* at higher levels than either Lin^- or Lin^+ cells. To further confirm the high level of *VASH1* expression in the HSC-enriched population, we identified HSCs by their ability to efflux Hoechst 33342 dye. This method defines an extremely small and haematopoietically potent subset of cells known as the side population (SP) (*20*, *21*). As shown in Fig. 1B, ~0.1% of BM cells are in the SP cell fraction, as previously reported (*20*). Treatment with verapamil, an inhibitor of ATP-binding cassette transporter superfamily pumps, resulted in the complete disappearance of this population. qRT–PCR analysis (Fig. 1D) indicated that SP cells express *VASH1* at much higher levels than cells from the main population (MP) or from the S and G2/M stages of the cell cycle. Lin^+ cells seemed not to express *VASH1* (Fig. 1C); also lymphocytes, myeloid cells and erythroid cells from BM and mononuclear cells (MNCs) from peripheral blood do not express *VASH1* (Fig. 1F). Although ECs derived from hind limb muscle of adult mice do express *VASH1* at levels 5-fold those of the HSC population in BM (Fig. 1E); nonetheless, we concluded that among HCs, *VASH1* is preferentially expressed in the HSC population and not in HPs or mature HCs in the BM in the steady state. Since it has been reported that VASH1 expression was upregulated upon the stimulation with VEGF or bFGF using HUVECs (*12*), we tried to observe whether the expression of VASH1 is upregulated in freshly isolated ECs from hind limb muscle of adult mice as used in Fig. 1E. Perhaps, by the technical limitation using primary ECs, we could not observe the upregulation of *VASH1* on primary ECs under stimulation with VEGF or bFGF.

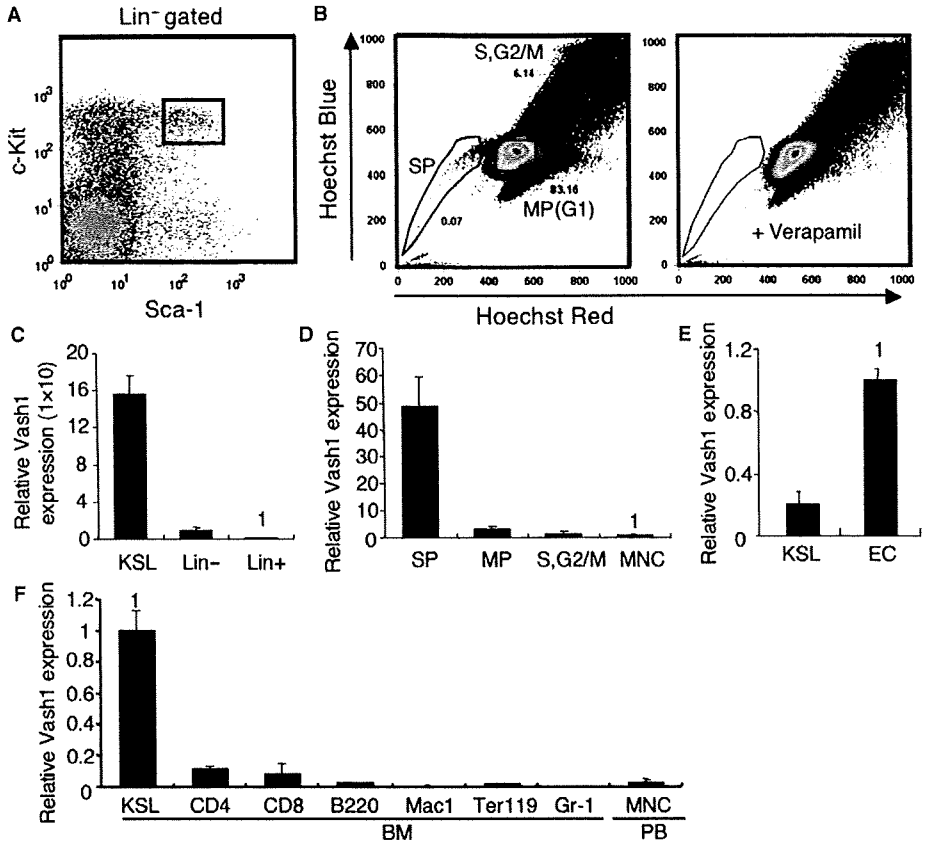

Fig. 1. **VASH1 expression in different haematopoietic lineages.** (A) Flow cytometric analysis of the HSC population. BM cells from 8-week-old mice were tested for the expression of Lin markers, c-Kit, Sca-1. Box indicates HSC population as $Lin^-c\text{-}Kit^+Sca\text{-}1^+$ cells. (B) Analysis of side population (SP) cells, main population (MP) cells and cells in the S, G2/M phase of the cell cycle from the BM of 8-week-old mice. The identification of SP cells was confirmed by their disappearance in the presence of Verapamil (right panel). (C–F) qRT–PCR for *VASH1* in several cells as indicated. Results (mean ± SD) are from three independently sorted sets of populations. (C) KSL HSC population, Lin^- haematopoietic progenitor-enriched population and Lin^+ mature haematopoietic cells from BM of 8-week-old mice. (D) SP cells, MP cells and cells in S,G2/M from adult BM. Mononuclear cells (MNCs) from whole BM were also used for comparison. (E) Comparison of *VASH1* expression by KSL cells as indicated in (A) and ECs from hind limb muscle of 8-week-old mice defined as $CD31^+CD45^-$ cells. (F) Comparison of *VASH1* expression in KSL cells with adult BM cells positive for several lineage markers as indicated. MNCs from peripheral blood (PB) from the same mice were also used for comparison.

Ischaemia Does Not Induce VASH1 in HCs—In the murine femoral artery occlusion hind limb ischaemia model, the expression of VEGF and bFGF is increased (*23*). It has been reported that VASH1 expression is induced by VEGF or bFGF in ECs (*12*) and that several HCs including the HSC population migrate into ischemic tissue from BM to support angiogenesis (*8*). We reasoned that if regulatory mechanisms for VASH1 expression are similar in ECs and HCs, the latter may also express VASH1 in ischemic tissues. To test this, $CD31^+CD45^-$ ECs, $CD31^-CD45^+$ HCs and $CD31^-CD45^-$ non-EC/non-HCs were isolated from hind limb muscle in the normoxic or hypoxic condition and *VASH1* expression was examined (Fig. 2A). Although we could not succeed to induce *VASH1* expression in the culture of primary ECs as described earlier, we found that hypoxia-induced *VASH1* expression in ECs, but neither in HCs nor non-ECs/non-HCs (Fig. 2B). Moreover, ischaemia in the hind limb did not affect *VASH1* expression by HCs residing in the BM (data not shown). These findings suggested that the regulatory mechanisms controlling *VASH1* expression in HCs and ECs are different.

VASH1 Expression is Induced in HPs After BM Ablation by 5-FU—5-FU treatment in mice induces BM ablation as a result of killing the cycling HSCs and HPs. However, surviving HSCs and HPs undergo acute expansion to produce a number of mature HCs. We therefore analysed whether BM suppression with 5-FU affects *VASH1* expression. It is well known that although the HSC population is decreased in mice during the first few days after 5-FU (150 mg/kg) injection, the population of cycling HSCs and HPs increases dramatically 4–6 days thereafter (*24*). We therefore sorted KSL cells, Lin^- cells, and Lin^+ cells from adult BM on day 7 after treatment with 5-FU (Fig. 2C and D). We found that *VASH1* expression in KSL cells and Lin^+ cells was not affected by 5-FU injection, but that it was now induced in Lin^- HPs to a similar extent as present in KSL cells (Fig. 2D). This was also confirmed at the protein level (Fig. 2E).

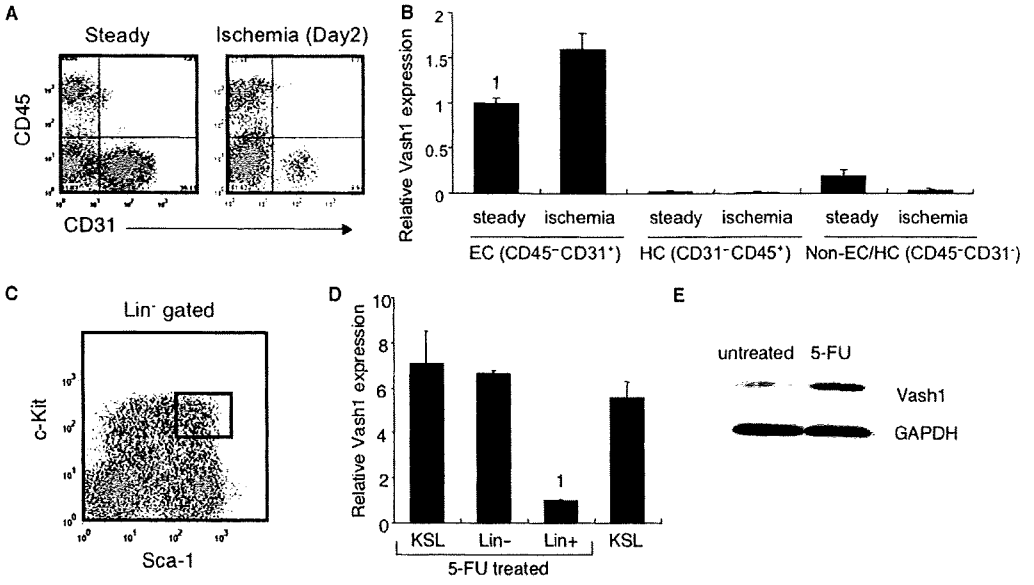

Fig. 2. **VASH1 expression on HCs in tissues under stress.** (A) Flow cytometric analysis of cells from hind limb muscle in the steady state and ischaemic state on the second day after femoral artery ligation. Cells were stained with CD31, an EC marker, and CD45, an HC marker. (B) qRT–PCR for *VASH1* expression in different cells sorted as shown in (A). Results (mean ± SD) are from three independently sorted sets of populations. C: BM cells from 10-week-old mice were isolated 7 days after systemic administration of 5-FU and tested for the expression of Lin markers, c-Kit, Sca-1 by flow cytometry. (D) qRT–PCR for levels of *VASH1* in KSL cells as shown in (C), Lin^- cells, and Lin^+ cells. KSL cells before 5-FU treatment are also used for comparison. (E) Western blotting for VASH1 expression. Lin^- haematopoietic progenitors from 10-week-old mice with or without 5-FU treatment were sorted and used for this analysis. GAPDH was used as an internal control.

VASH1 and VEGFR2 Expression in HPs After BM Ablation by 5-FU—It has been reported that HSCs and HPs express VEGFR2/Flk1, a receptor for VEGF, and that VEGF induces the expansion of $VEGFR2^+$ HPs (*25*). VEGF is upregulated after BM suppression (*26*). Moreover, knockdown of *VASH1* mRNA suggested that attenuation of VASH1 expression leads to a significant elevation in the level of *VEGFR2* mRNA in ECs (*17*). Therefore, it is possible that upregulated VASH1 in HPs suppresses VEGFR2 expression. Therefore, Lin^- BM HPs in the steady state and after 5-FU treatment were sorted into $VEGFR2^+$ and $VEGFR2^-$ populations (Fig. 3A) and their *VASH1* expression quantified. It was found that $VEGFR2^+$ cells expressed *VASH1* at higher levels than $VEGFR2^-$ cells in the steady state as well as after treatment with 5-FU (Fig. 3B). However, $VEGFR2^-$ cells from 5-FU-treated animals expressed more *VASH1* than those from controls (Fig. 3B). Moreover, cells very strongly positive for VEGFR2, which were present in controls, disappeared after 5-FU treatment (Fig. 3A, box in left panel). This suggests that VASH1 induction in $VEGFR2^{high}$ HPs after 5-FU treatment may attenuate the expression of VEGFR2, which may shift $VEGFR2^{high}$ cells to $VEGFR2^{low/-}$ cells.

Attenuation of Vash1 Expression Induces Proliferation of Leukaemia Cells—To seek models for understanding the role of VASH1 induction in HPs after BM ablation, we searched for VASH1-expressing HC lines. Of three human acute myeloblastic leukaemia (AML) cell lines, two (KG1a and THP1) strongly expressed *VASH1A*, but none of four acute lymphoid leukaemia (ALL) cell lines did so (Fig. 4A and B). In this experiment, we used

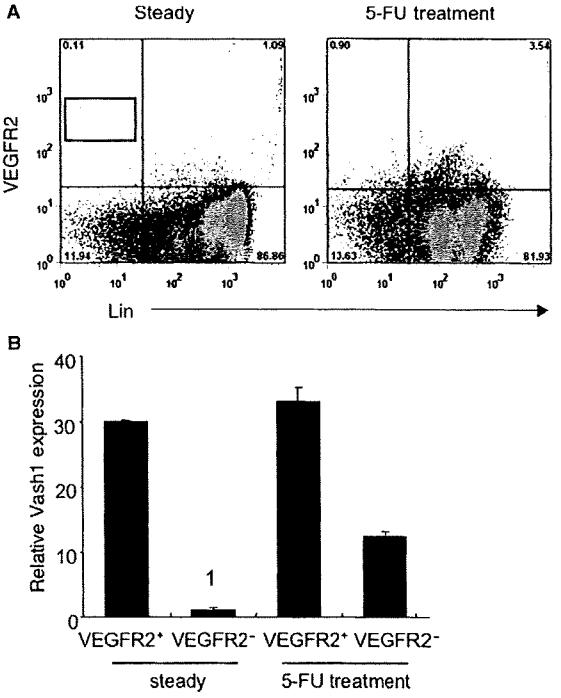

Fig. 3. **VEGFR2 expression by haematopoietic progenitors after treatment with 5-FU.** (A) BM cells from 10-week-old mice before and after (7 days) treatment with 5-FU were stained for lineage markers and antibody against VEGFR2. Note that $Lin^-VEGFR2^{high}$ cells indicated by the box disappeared after treatment with 5-FU. (B) qRT–PCR for *VASH1* in different cell populations from adult BM before and after treatment with 5-FU as shown in (A).

A

Cell line	Class
KG1a	AM(M0)
HL60	AML(M3)
THP-1	AML(M5)
MOLT-4	T-ALL
SKW3	T-ALL
BALL-1	B-ALL
NALM6	B-ALL

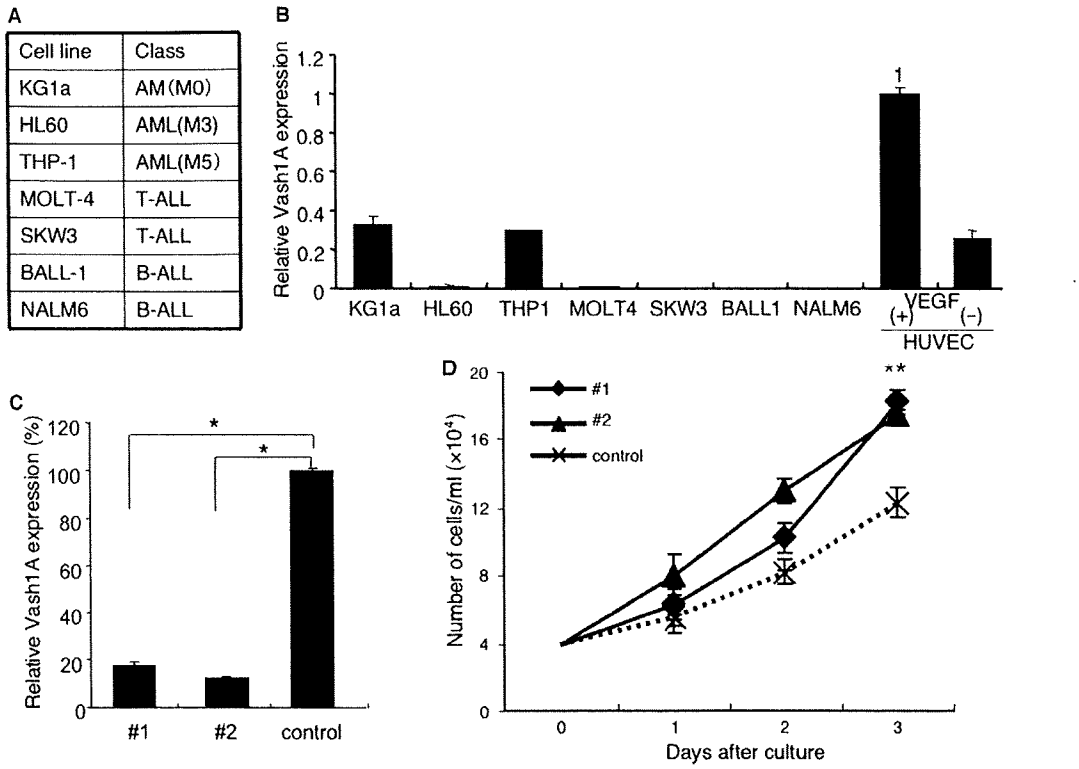

Fig. 4. **Expression of VASH1A in leukaemic cell lines.** (A) Leukaemic cell lines used in this experiment. (B) qRT–PCR for *VASH1A* in different leukaemic cells. HUVECs stimulated with (+) or without (−) VEGF were used as positive controls. (C) qRT-PCR for *VASH1A* after silencing by two RNAis (#1 and #2) or a control RNAi (control). $^{*}P<0.05$ ($n=3$, mean ± SD). (D) Cell growth after introduction of RNAi as described in (C). $^{**}P<0.05$ ($n=3$, mean ± SD).

HUVECs as a positive control and confirmed that VEGF induces *VASH1A* expression in HUVECs as previously reported (*12*) (Fig. 4B).

As it has been suggested the existence of alternatively splicing short forms of *VASH1A* termed *VASH1B*, we detected *VASH1B* in these two leukaemia cell line (KG1a and THP1) at a similar extent with *VASH1A* (data not shown).

Using RNAi methodology targeting two different cording regions of the human *Vash1* mRNA sequence, we then tested the effect of blocking VASH1 on cell growth. For reasons that remain unclear, this approach was not successful technically with KG1a cells, but *VASH1A* expression in THP1 cells could be greatly attenuated in this way (Fig. 4C). Proliferation of cells in which *VASH1A* had been knocked down was significantly greater than in controls, suggesting that attenuation of VASH1A expression enhances cell proliferation (Fig. 4D).

DISCUSSION

It has been reported that VASH1 expression is induced in ECs after stimulation with VEGF or bFGF and that this factor then inhibits their proliferation and migration. Therefore, it has been suggested that VASH1 acts as a negative feedback regulator for angiogenesis to inhibit overgrowth of blood vessels. In the BM, SP cells are suggested to be the most immature HSC population that can be serially transplantable into lethally irradiated mice. As most SP cells are dormant and most likely adhere to osteoblasts in the BM (*21*), it is possible that VASH1 inhibits SP cell-cycle progression in such BM niches. To address this, an HSC-specific conditional knock-out of the *VASH1* gene will be required. However, thus far molecules specifically expressed on SP cells have not been well documented, with the exception of ABCG2, an ABC transporter. Therefore, we propose that our present data identifying a novel molecule expressed on SP cells will be useful at least as a marker.

It is of note that VASH1 expression was induced in HPs, but not HSCs, during recovery from BM ablation. It had been considered that surviving HSCs in the BM start to self-renew and subsequently HPs derived from these HSCs acutely proliferate. However, in HSC division, it is not clear whether a single HSC gives rise to two HSC by symmetrical cell division or whether one HSC and one progenitor are produced by asymmetric cell division. Of course, it is possible that both types of cell division occur, but the mechanisms responsible for controlling when HSCs stop dividing remain obscure. If VASH1 has a role in maintaining HSC pool size in the BM by inhibiting cell growth, it would be expected that VASH1 expression should be induced in this population during recovery after BM ablation. However, VASH1 expression in HSCs was not affected by treatment

with 5-FU, suggesting that their cell division occurs very early after ablation of the BM and stops soon after giving rise to daughter progenitor cells.

During the recovery stage, HPs proliferate acutely; however, their cell division needs to be downregulated again after sufficient mature HCs have been generated. The mechanism responsible for this negative feedback regulation has thus far eluded identification. Our results presented here suggest that VASH1 might be a one of the negative regulators active at the final stage of acute recovery following BM ablation, because knockdown of the *VASH1A* gene-enhanced proliferation of VASH1A$^+$ cells from leukaemic lines.

Currently, it is thought that the expression of VASH1 and VEGFR2 is reciprocally cross-regulated in ECs (*17*). Attenuation of VEGFR2 expression by VASH1 may reduce responsiveness to VEGF, resulting in inhibition of angiogenesis. In the present study, HPs highly expressing VEGFR2 disappeared during recovery from BM ablation. It has been reported that VEGF promotes proliferation of HPs (*25*). Therefore, upregulation of VASH1 on HPs may reduce the expression of VEGFR2 as a means of negative feedback regulation of HP proliferation. Regulation of VEGFR2 expression by HPs may be part of the mechanism controlling the function of VASH1 in haematopoiesis. However, VEGFR2$^+$ HPs represent a very minor population among HPs. Therefore, other molecules must be involved in the negative regulation of cell growth in haematopoiesis. To understand the precise mechanism, targeted disruption of the VASH1 gene in HPs is required. This would enable the determination of the precise function of VASH1 in HP proliferation and negative feedback regulation to maintain HP pool size.

ACKNOWLEDGEMENT

We thank Mrs K. Fukuhara and N. Fujimoto for technical assistance.

FUNDING

This work was partly supported by the Japanese Ministry of Education, Culture, Sports, Science and Technology and the Japan Society for Promotion of Science.

CONFLICT OF INTEREST

None declared.

REFERENCES

1. Choi, K., Kennedy, M., Kazarov, A., Papadimitriou, J.C., and Keller, G. (1998) A common precursor for hematopoietic and endothelial cells. *Development* **125**, 725–732
2. Nishikawa, S.I., Nishikawa, S., Kawamoto, H., Yoshida, H., Kizumoto, M., Kataoka, H., and Katsura, Y. (1998) *In vitro* generation of lymphohematopoietic cells from endothelial cells purified from murine embryos. *Immunity* **8**, 761–769
3. Yamada, Y. and Takakura, N. (2006) Physiological pathway of differentiation of hematopoietic stem cell population into mural cells. *J. Exp. Med.* **203**, 1055–1065
4. Sata, M., Saiura, A., Kunisato, A., Tojo, A., Okada, S., Tokuhisa, T., Hirai, H., Makuuchi, M., Hirata, Y., and Nagai, R. (2002) Hematopoietic stem cells differentiate into vascular cells that participate in the pathogenesis of atherosclerosis. *Nat. Med.* **8**, 403–409
5. Sugiyama, T., Kohara, H., Noda, M., and Nagasawa, T. (2006) Maintenance of the hematopoietic stem cell pool by CXCL12-CXCR4 chemokine signaling in bone marrow stromal cell niches. *Immunity* **25**, 977–988
6. Avecilla, S.T., Hattori, K., Heissig, B., Tejada, R., Liao, F., Shido, K., Jin, D.K., Dias, S., Zhang, F., Hartman, T.E., Hackett, N.R., Crystal, R.G., Witte, L., Hicklin, D.J., Bohlen, P., Eaton, D., Lyden, D., de Sauvage, F., and Rafii, S. (2004) Chemokine-mediated interaction of hematopoietic progenitors with the bone marrow vascular niche is required for thrombopoiesis. *Nat. Med.* **10**, 64–71
7. Takakura, N., Watanabe, T., Suenobu, S., Yamada, Y., Noda, T., Ito, Y., Satake, M., and Suda, T. (2000) A role for hematopoietic stem cells in promoting angiogenesis. *Cell* **102**, 199–209
8. Takakura, N. (2006) Role of hematopoietic lineage cells as accessory components in blood vessel formation. *Cancer Sci.* **97**, 568–574
9. Coussens, L.M., Raymond, W.W., Bergers, G., Laig-Webster, M., Behrendtsen, O., Werb, Z., Caughey, G.H., and Hanahan, D. (1999) Inflammatory mast cells up-regulate angiogenesis during squamous epithelial carcinogenesis. *Genes Dev.* **13**, 1382–1397
10. Hiratsuka, S., Nakamura, K., Iwai, S., Murakami, M., Itoh, T., Kijima, H., Shipley, J.M., Senior, R.M., and Shibuya, M. (2002) MMP9 induction by vascular endothelial growth factor receptor-1 is involved in lung-specific metastasis. *Cancer Cell* **2**, 289–300
11. Ribatti, D., Presta, M., Vacca, A., Ria, R., Giuliani, R., Dell'Era, P., Nico, B., Roncali, L., and Dammacco, F. (1999) Human erythropoietin induces a pro-angiogenic phenotype in cultured endothelial cells and stimulates neovascularization in vivo. *Blood* **93**, 2627–2636
12. Watanabe, K., Hasegawa, Y., Yamashita, H., Shimizu, K., Ding, Y., Abe, M., Ohta, H., Imagawa, K., Hojo, K., Maki, H., Sonoda, H., and Sato, Y. (2004) Vasohibin as an endothelium-derived negative feedback regulator of angiogenesis. *J. Clin. Invest.* **114**, 898–907
13. Nimmagadda, S., Geetha-Loganathan, P., Pröls, F., Scaal, M., Christ, B., and Huang, R. (2007) Expression pattern of Vasohibin during chick development. *Dev. Dyn.* **236**, 1385–1362
14. Sonoda, H., Ohta, H., Watanabe, K., Yamashita, H., Kimura, H., and Sato, Y. (2006) Multiple processing forms and their biological activities of a novel angiogenesis inhibitor vasohibin. *Biochem. Biophys. Res. Commun.* **342**, 640–646
15. Kern, J., Bauer, M., Rychli, K., Wojta, J., Ritsch, A., Gastl, G., Gunsilius, E., and Untergasser, G. (2008) Alternative splicing of vasohibin-1 generates an inhibitor of endothelial cell proliferation, migration, and capillary tube formation. *Arterioscler. Thromb. Vasc. Biol.* **28**, 478–484
16. Shibuya, T., Watanabe, K., Yamashita, H., Shimizu, K., Miyashita, H., Abe, M., Moriya, T., Ohta, H., Sonoda, H., Shimosegawa, T., Tabayashi, K., and Sato, Y. (2006) Isolation and characterization of vasohibin-2 as a homologue of VEGF-inducible endothelium-derived angiogenesis inhibitor vasohibin. *Arterioscler. Thromb. Vasc. Biol.* **26**, 1051–1057
17. Shen, J., Yang, X., Xiao, W.H., Hackett, Y., Sato, Y., and Campochiaro, P.A. (2006) Vasohibin is up-regulated by VEGF in the retina and suppresses VEGF receptor 2 and retinal neovascularization. *FASEB J.* **20**, 723–725
18. Yamashita, H., Abe, M., Watanabe, K., Shimizu, K., Moriya, T., Sato, A., Satomi, S., Ohta, H., Sonoda, H., and Sato, Y. (2006) Vasohibin prevents arterial neointimal formation through angiogenesis inhibition. *Biochem. Biophys. Res. Commun.* **345**, 919–925

19. Yoshinaga, K., Ito, K., Moriya, T., Nagase, S., Takano, T., Niikura, H., Yaegashi, N., and Sato, Y. (2008) Expression of vasohibin as a novel endothelium-derived angiogenesis inhibitor in endometrial cancer. *Cancer Sci.* **99**, 914–919
20. Goodell, M.A., Brose, K., Paradis, G., Conner, A.S., and Mulligan, R.C. (1996) Isolation and functional properties of murine hematopoietic stem cells that are replicating *in vivo*. *J. Exp. Med.* **183**, 1797–1806
21. Arai, F., Hirao, A., Ohmura, M., Sato, H., Matsuoka, S., Takubo, K., Ito, K., Koh, G.Y., and Suda, T. (2004) Tie2/angiopoietin-1 signaling regulates hematopoietic stem cell quiescence in the bone marrow niche. *Cell* **118**, 149–161
22. Kidoya, H., Ueno, M., Yamada, Y., Mochizuki, N., Nakata, M., Yano, T., Fujii, R., and Takakura, N. (2008) Spatial and temporal role of the apelin/APJ system in the caliber size regulation of blood vessels during angiogenesis. *EMBO J.* **27**, 522–534
23. Kinnaird, T., Stabile, E., Burnett, M.S., and Epstein, S.E. (2004) Bone-marrow-derived cells for enhancing collateral development: mechanisms, animal data, and initial clinical experiences. *Circ. Res.* **95**, 354–363
24. Darnowski, J.W. and Handschumacher, R.E. (1985) Tissue-specific enhancement of uridine utilization and 5-fluorouracil therapy in mice by benzylacyclouridine. *Cancer Res.* **45**, 5364–5368
25. Smith, S.L., Agbemadzo, B., Reems, J.A., Tyler, T., Kiss, J., and Moldwin, R.L. (2000) Expansion of CD34+KDR+cells in cord blood after culture with TPO, FLT-3L, SCF, and VEGF. *Exp. Hematol.* **28**, 94
26. Rafii, S., Avecilla, S., Shmelkov, S., Shido, K., Tejada, R., Moore, M.A., Heissig, B., and Hattori, K. (2003) Angiogenic factors reconstitute hematopoiesis by recruiting stem cells from bone marrow microenvironment. *Ann. NY Acad. Sci.* **996**, 49–60

EXPERIMENTAL CELL RESEARCH 316 (2010) 775-788

available at www.sciencedirect.com

ScienceDirect

www.elsevier.com/locate/yexcr

Research Article

Impairment of VEGF-A-stimulated lamellipodial extensions and motility of vascular endothelial cells by chondromodulin-I, a cartilage-derived angiogenesis inhibitor

Shigenori Miura[a], *Kaori Mitsui*[b], *Takahiro Heishi*[c], *Chisa Shukunami*[a], *Kiyotoshi Sekiguchi*[d], *Jun Kondo*[e], *Yasufumi Sato*[c], *Yuji Hiraki*[a,*]

[a]*Department of Cellular Differentiation, Institute for Frontier Medical Sciences, Kyoto University, 53 Shogoin-Kawahara-cho, Sakyo-ku, Kyoto 606-8507, Japan*
[b]*Research and Development Division, Science and Technology Research Center Inc., Mitsubishi Chemical Group, Kanagawa 227-8502, Japan*
[c]*Department of Vascular Biology, Institute of Development, Aging, and Cancer, Tohoku University, Sendai 980-8575, Japan*
[d]*Laboratory of Extracellular Matrix Biochemistry, Institute for Protein Research, Osaka University, 3-2 Yamadaoka, Suita, Osaka 565-0871, Japan*
[e]*Advanced Medical Research Laboratory, Research Division, Mitsubishi Tanabe Pharma Corporation, Kanagawa 227-0033, Japan*

ARTICLE INFORMATION

Article Chronology:
Received 20 July 2009
Revised version received
15 November 2009
Accepted 14 December 2009
Available online 21 December 2009

Keywords:
Chondromodulin-I
VEGF-A
Angiogenesis inhibitor
Vascular endothelial cell
Cell migration

ABSTRACT

Chondromodulin-I (ChM-I) is a cartilage-derived angiogenesis inhibitor that has been identified as inhibitory to the growth activity of vascular endothelial cells. In our present study, we demonstrate the anti-angiogenic activity of recombinant human ChM-I (rhChM-I) in mouse corneal angiogenesis and examine its action. We focus on the VEGF-A-induced migration of vascular endothelial cells, a critical regulatory step in angiogenesis. In a modified Boyden chamber assay, nanomolar concentrations of rhChM-I inhibited the chemotactic migration of human umbilical vein endothelial cells (HUVECs) induced by VEGF-A as well as by FGF-2 and IGF-I. The ChM-I action was found to be endothelial cell-specific and independent of cell adhesions. Time-lapse analysis further revealed that rhChM-I markedly reduces VEGF-A-stimulated motility of HUVECs and causes frequent alterations of the moving front due to the appearance of multiple transient protrusions. This action involved the inhibition of cell spreading and the disrupted reorganization of the actin cytoskeleton upon VEGF-A stimulation. Consistent with these observations, rhChM-I was found to significantly reduce the activity of Rac1/Cdc42 during cell spreading, and the VEGF-A-induced Rac1 activity but not its basal activity in quiescent cells. Taken together, our present data suggest that ChM-I impairs the VEGF-A-stimulated motility of endothelial cells by destabilizing lamellipodial extensions.

Introduction

Angiogenesis, the formation of new capillaries from pre-existing blood vessels, is critical for various physiological processes and also the progression of pathological disorders including rheumatoid arthritis, tumor growth, and metastasis [1]. Basement membranes are amorphous dense sheet-like structures of extracellular matrix (ECM) that support the growth of epithelial and

* *Corresponding author.* Fax: +81 75 751 4633.
E-mail address: hiraki@frontier.kyoto-u.ac.jp (Y. Hiraki).

0014-4827/$ - see front matter © 2009 Elsevier Inc. All rights reserved.
doi:10.1016/j.yexcr.2009.12.009

endothelial cells and enable them to function as an anti-angiogenic barrier against invading vasculature from the underlying mesenchymal tissue [2]. During the past decade, a number of endogenous inhibitors of angiogenesis have been identified, most of which are classified as cryptic inhibitors that are encoded within specific domains of larger ECM components and are cleaved by degradation during the remodeling of basement membranes. Examples include endostatin, arresten, canstatin, and tumstatin [3,4]. In contrast to the epithelium, mesenchymal tissues are generally well vascularized and permissive for vascularization. Hence, most organ stroma and connective tissues readily allow the ingrowth of blood vessels upon stimulation by inflammation or hypoxia, in which vascular endothelial growth factor-A (VEGF-A) plays a central role as a pro-angiogenic cytokine. Hyaline cartilage is a connective tissue that contains a large amount of viscoelastic ECM but is exceptionally avascular and highly resistant to neovascularization as well as tumor invasion.

Chondromodulin-I (ChM-I) is a 25-kDa glycoprotein that was originally purified from the guanidine extracts of fetal bovine cartilage [5,6]. Purified bovine ChM-I inhibits the proliferation and tube morphogenesis of vascular endothelial cells *in vitro* as well as angiogenesis in the chick chorioallantoic membrane [5–9]. The localization of ChM-I transcripts has been shown to be specific to the avascular domains of mesenchymal tissues, including certain ocular tissues and cardiac valves as well as cartilage [10–14]. ChM-I null mice develop pathological angiogenesis in the cardiac valve with age, suggesting a function for ChM-I as an endogenous angiogenesis inhibitor that ensures avascularity in certain connective tissues [13,15].

Sprouting angiogenesis proceeds via several well-characterized stages [16]. Upon activation by pro-angiogenic stimuli, endothelial cells first begin to release matrix metalloproteinases that degrade the basement membrane to enable migration into the perivascular space and towards angiogenic stimuli. This is followed by the proliferation of endothelial cells and formation of solid sprouts. Finally, tube morphogenesis restructures the sprouts into a lumen lined by endothelial cells. We previously demonstrated that ChM-I inhibits both DNA synthesis and tube morphogenesis in vascular endothelial cells [7–9]. In our present study, using recombinant human ChM-I (rhChM-I), we studied the actions of ChM-I on the chemotactic migration and motile activities of vascular endothelial cells.

Materials and methods

Antibodies and reagents

Antibodies against paxillin, focal adhesion kinase (FAK), phospho-FAK (pY397), Rac1, and Cdc42 were purchased from BD Transduction Laboratories (Franklin Lakes, NJ). Anti-β-actin monoclonal antibody (AC-15) was obtained from Sigma (St. Louis, MO). Rat anti-mouse CD31 and rabbit anti-mouse LYVE-1 antibodies were obtained from Research Diagnosis Inc. (Flanders, NJ) and Acris Antibodies GmbH (Hiddenhausen, Germany), respectively. Alexa Fluor 594-conjugated phalloidin and Alexa Fluor 488-conjugated goat anti-mouse IgG antibody were purchased from Molecular Probes (Eugene, OR). Recombinant human endostatin, phorbol 12-myristate 13-acetate (PMA), and pertussis toxin (PTX) were obtained from Sigma. Sphingosine 1-phosphate (S1P) was obtained from BIOMOL (Plymouth Meeting, PA). Recombinant human VEGF-A_{165}, fibroblast growth factor-2 (FGF-2), and insulin-like growth factor-I (IGF-I) were purchased from R&D Systems (Minneapolis, MN). Pharmacological inhibitor, SU5402, was obtained from Calbiochem (La Jolla, CA).

Expression and purification of recombinant human ChM-I

Recombinant human ChM-I (rhChM-I, corresponding to the region Glu^{215}-Val^{334} of the human ChM-I precursor) was expressed as an N-terminally FLAG tagged protein using the pCAGGS expression vector (a generous gift of Dr. J. Miyazaki, Osaka University Graduate School of Medicine, Japan) [17], as described previously [18]. The expression of rhChM-I was performed under serum-free conditions using the FreeStyle™ 293 Expression system (Invitrogen, Carlsbad, CA) and rhChM-I was purified from the culture medium using anti-FLAG M2 affinity gel (Sigma) according to the manufacturer's instructions. This single-step purification yielded bioactive rhChM-I with an approximate purity of 70% as determined by BCA Protein Assay Kit (Pierce, Rockford, IL) and western blotting using an anti-ChM-I antibody. CHO-hChM-I was prepared from the culture media of CHO cells transfected with human ChM-I precursor cDNA, as described previously [9].

Mouse corneal micropocket assay

The mouse corneal micropocket assays were performed as described previously [19]. Briefly, 4-week-old male BALB/c mice (Charles River Laboratories Japan, INC., Yokohama, Japan) were deeply anesthetized, and 0.3 μg poly-2-hydroxyethyl methacrylate (HEME) pellets (Sigma) containing either vehicle or 160 ng (an optimized dose for the induction of corneal angiogenesis) of VEGF-A ($VEGF_{165}$) (Sigma) with or without rhChM-I (34 ng, a maximal dose that could be included in the HEME pellet without disturbing its solidification.) were implanted in the corneas. Fourteen days after pellet inoculation, the corneas were excised, washed in PBS, and fixed in acetone at 4 °C for 30 min. After three additional washings in PBS and blocking with 1% BSA in PBS for 1 h, the corneas were stained overnight at 4 °C with rat anti-mouse CD31 antibody (1:500) and rabbit anti-mouse LYVE1 antibody (1:500). On day 2, the corneas were washed, and secondary antibody reactions were performed using Alexa Fluor 488 donkey anti-rat IgG (1:1000) and Alexa Fluor 568 goat anti-rabbit IgG (1:1000) for 6 h at 4 °C. After a final washing, the sections were covered with fluorescent mounting medium (DakoCytomation Inc., Carpinteria, CA). Double-stained whole-mount sections were visualized using a FluoView FV1000 confocal microscope (Olympus Corp., Tokyo, Japan). Blood vessels were positive for CD31 and negative for LYVE1. Lymphatic vessels were double positive for CD31 and LYVE1. The area covered by blood and lymphatic vessels was measured in five random fields for each animal using NIH ImageJ software (ver. 1.39u).

Cell culture

Human umbilical vein endothelial cells (HUVECs; Lonza, Walkersville, MD) at passages 4–7 and bovine aortic endothelial cells (BAECs; Cell Applications Inc.) at passages 3–5 were grown to subconfluence and used in the current experiments. Cells of the